Noise estimation of SDE from a single data trajectory

Munawar Ali * Purba Das[†] Qi Feng[‡] Liyao Gao[§] Guang Lin[¶]

Abstract

In this paper, we propose a data-driven framework for model discovery of stochastic differential equations (SDEs) from a single trajectory, without requiring the ergodicity or stationary assumption on the underlying continuous process. By combining (stochastic) Taylor expansions with Girsanov transformations, and using the drift function's initial value as input, we construct drift estimators while simultaneously recovering the model noise. This allows us to recover the underlying $\mathbb P$ Brownian motion increments. Building on these estimators, we introduce the first stochastic Sparse Identification of Stochastic Differential Equation (SSISDE) algorithm, capable of identifying the governing SDE dynamics from a single observed trajectory without requiring ergodicity or stationarity. To validate the proposed approach, we conduct numerical experiments with both linear and quadratic drift—diffusion functions. Among these, the Black—Scholes SDE is included as a representative case of a system that does not satisfy ergodicity or stationarity.

Keywords: SSISDE, Sparse regression, SINDy, Risk-neutral Brownian motion, Physical Brownian motion, Stochastic Taylor expansion, Girsanov transformation, Signature model, Drift and diffusion estimate, Quadratic variation, Stratonovich and Itô SDE.

2000 AMS Mathematics subject classification: 62P05, 37M10, 60H10, 60G17, 65C30.

1 Introduction

Stochastic differential equations (SDEs) are fundamental tools for modeling systems with inherent randomness, but estimating the underlying continuous dynamics from observed discrete data remains both challenging and important. The initial development in this area was closely tied to applications in economics and finance, including Anderson (1959); Merton (1980); Melino (1994); Aït-Sahalia (1996); Hansen and Scheinkman (1993); Hansen et al. (1998); Stanton (1997); Duffie and Glynn (2004), among many others. A central challenge in working with stochastic differential equations (SDEs) is that, in practice, one typically only observes the process at discrete time points, while the key quantities driving the dynamics—such as the drift and diffusion coefficients or even the underlying noise—remain unknown. Recovering both the system parameters and the latent noise process from such partial information is therefore of significant theoretical and practical interest, particularly in stochastic modeling and statistical inference Kutoyants (2013); Kessler (1997).

In this paper, we study the problem of recovering the drift and diffusion functions from a high-frequency single realization of a continuous-time stochastic process $\{X_t\}_{t\geq 0}$ governed by the Itô SDE

$$dX_t = \mu(X_t)dt + \sigma(X_t)dB_t^{\mathbb{P}},\tag{1}$$

where μ and σ denote the drift and diffusion functions, respectively, and $B^{\mathbb{P}}$ is a canonical Brownian motion under the physical measure \mathbb{P} , i.e. the filtration is generated by the X_t . Classical approaches to estimating μ and σ include kernel-based estimators Lamouroux and Lehnertz (2009); Florens-Zmirou (1989); Stanton (1997), maximum likelihood methods Bibby and Sørensen (1995); Dacunha-Castelle and Florens-Zmirou (1986); Aït-Sahalia (2002), and local polynomial regression Fan and Zhang (2003). These methods, however, typically rely on ergodicity or stationarity of the underlying process or the availability of repeated observations. More recent developments employ tools from empirical process theory and martingale estimation to handle high-frequency

^{*}Department of Mathematics, Florida State University, Tallahassee, 32306; email: ma22bm@fsu.edu.

[†]Department of Mathematics, King's College London, London, UK; email: purba.das@kcl.ac.uk.

[‡]Department of Mathematics, Florida State University, Tallahassee, 32306; email: qfeng2@fsu.edu. This author is partially supported by the National Science Foundation under grant #DMS-2420029.

[§]Department of Computer Science, University of Washington, Seattle, WA 98195.

^{*}Department of Mathematics, Purdue University, West Lafayette, IN; email: guanglin@purdue.edu. This author is partially supported by the National Science Foundation (NSF) (DMS-2533878, DMS-2053746, DMS-2134209, ECCS-2328241, CBET-2347401, and OAC-2311848), and DOE Office of Science Advanced Scientific Computing Research program DE-SC0023161, and DOE-Fusion Energy Science, under grant number: DE-SC0024583.

data Dalalyan and Reiß (2007); Comte et al. (2007), but these approaches still require strong structural assumptions such as stationarity, ergodicity, or multiple sample paths. These assumptions are often unrealistic in a financial context; for example, if one assumes the classical Black-Scholes model for a price path, then the price path is not ergodic.

On the other hand, in the absence of noise in (1), the deterministic dynamics can be analyzed in much greater detail. Particularly, the discovery of a deterministic dynamical system, obtained by setting $\sigma \equiv 0$ in equation (1),

$$\dot{\mathbf{x}}(t) = \mu(\mathbf{x}(t)),\tag{2}$$

can be formulated as a symbolic regression problem of the following form:

$$\dot{\mathbf{X}} = \Theta(\mathbf{X})\Xi,\tag{3}$$

where $\Theta(\mathbf{X})$ denotes the function library matrix composed of p candidate terms, typically including polynomials, trigonometric functions, exponentials, and sinusoidal functions. The unknown sparse matrix Ξ $(\xi_1 \ \xi_2 \ \cdots \ \xi_n) \in \mathbb{R}^{p \times n}$ encodes the active terms and thus determines the governing dynamics. The input X denotes the vector of data snapshots over the discrete time grid. The state snapshots $\mathbf{X}(t)$ are observed in discrete time instances, and their temporal derivatives $\mathbf{X}(t)$ are obtained from data. The identification/estimation of the vector Ξ is called regression. Over the past decades, significant efforts have been devoted to data-driven model discovery. Early approaches include symbolic regression Koza (1994) for uncovering the structure of ODEs Schmidt and Lipson (2009); Bongard and Lipson (2007). Subsequent advances introduced sparse regression techniques for identifying ODEs Mangan et al. (2016); Brunton et al. (2016); Mangan et al. (2017) and PDEs Rudy et al. (2017); Zhang and Lin (2018); Schaeffer et al. (2017) with constant coefficients, along with group sparsity and sequentially grouped threshold ridge regression to capture spatial- or temporal-dependent coefficients Yuan and Lin (2006); Friedman et al. (2010); Casella et al. (2010). More recently, symbolic regression models Brunton et al. (2016); Udrescu and Tegmark (2020); Chen et al. (2021) have focused on extracting analytic expressions from large datasets, offering greater interpretability. Recent developments in data-driven frameworks further include the use of rough path theory and signature methods Semnani et al. (2025), as well as sparse identification of nonlinear stochastic dynamics Boninsegna et al. (2018); Wanner and Mezić (2024). Sparse learning has also proven highly effective in a broad range of applications in engineering, including fluid dynamics Bai et al. (2017), plasma dynamics Kaptanoglu et al. (2023), nonlinear optics Ermolaev et al. (2022), mesoscale ocean closures Zanna and Bolton (2020), and computational chemistry Harirchi et al. (2020).

However, the stochastic extension of Sparse Identification of Nonlinear Dynamics (SINDy) is highly nontrivial, due to the fact that SINDy fundamentally requires computing the temporal derivatives, which are known to be sensitive to noise. Additionally, it is also mathematically unclear on how to identify the drift μ and the underlying 'rough' noise term $B^{\mathbb{P}}$ of (1), from a single path observation on a finite time interval Stevens-Haas et al. (2024); Boninsegna et al. (2018); Wanner and Mezić (2024). In contrast to the current literature concerning these problems, our method is data-driven, does not assume strong regularity conditions, ergodic or stationary properties of the underlying process, and also uses a single path of the SDE. Our technique also extracts the noise from the finite sample data. Our proposed new methodology combines stochastic analysis, approximation techniques, and linear regression, with the only major assumption being the knowledge of the drift coefficient at the initial time point. Building on the Itô-Stratonovich correspondence Øksendal (2003), we approximate the drift and diffusion terms using Taylor expansions and reformulate the SDE in terms of iterated integrals. These iterated integrals, also known as signatures in rough path theory Lyons (1998); Friz and Victoir (2010), have recently been developed into powerful signature models in finance Arribas (2018); Cuchiero et al. (2023); Bayer et al. (2023); Cuchiero et al. (2025). A crucial step in our approach leverages Girsanov's theorem Girsanov (1960); Karatzas and Shreve (1991) to transform the dynamics into a representation involving iterated integral type terms, which admit explicit computation Lyons (1998); Kidger and Lyons (2020), and the convergence rate of such terms are well explored. Through further simplifications, inspired by the structure of the Black-Scholes model Black and Scholes (1973), we obtain a representation suitable for regression-based identification of drift, diffusion, and the underlying Brownian motion paths. Using the estimated increment of \mathbb{P} Brownian motion and the data snapshot of X, we introduce a new stochastic symbolic regression problem,

$$\arg \min_{\Xi_{\sigma},\Xi_{\mu}} ||\Delta X - \Theta_{\mu}(X)\Xi_{\mu}\Delta t - \Theta_{\sigma}(X)\Xi_{\sigma}\Delta B_{t}^{\mathbb{P}}||_{2}^{2} + \mathcal{R}_{\alpha,\rho}(\Xi_{\mu},\Xi_{\sigma}), \tag{4}$$

where the first loss is to fit the model, and the second promotes sparsity through regularization.

The remainder of the paper is organized as follows. Section 2 formulates the problem, introduces the proposed algorithms, and reviews the necessary background on SDEs. Section 3 develops the stochastic sparse identification of SDEs (SSISDE) framework for regression-based estimation, enabling the simultaneous recovery of the drift, diffusion, and underlying noise. Section 4 presents numerical experiments illustrating the effectiveness of the proposed method, including an application to the Black–Scholes SDE, which notably does not satisfy the ergodicity and stationary conditions.

2 Background and problem formulation

Let B be the Brownian motion defined on the canonical probability space $(\Omega, \mathcal{F}, \{\mathcal{F}\}_{t\geq 0}, \mathbb{P})^1$. We assume our time series data $X_{t_0}, X_{t_1}, \dots X_{t_N}$ comes from the underlying continuous process X_t which follows a stochastic differential equation (under the physical measure) of the form

$$dX_t = \mu(X_t)dt + \sigma(X_t)dB_t^{\mathbb{P}}. (5)$$

Note that the underlying process (5) does not always process a unique solution for general drift (μ) and diffusion (σ) coefficients. Nonetheless, under nominal assumptions (Lipchitz continuity and linear growth) on the drift (μ) and diffusion (σ) coefficient, one can ensure the existence and uniqueness of such a solution (Karatzas and Shreve, 1991, Chapter 5).

The first main goal of this paper is to estimate simultaneously the underlying noise vector $(B_{t_0}^{\mathbb{P}}, B_{t_0}^{\mathbb{P}}, \cdots B_{t_N}^{\mathbb{P}})$, the drift vector $(\mu(X_{t_0}), \mu(X_{t_1}), \cdots \mu(X_{t_N}))$, and the diffusion vector $(\sigma(X_{t_0}), \sigma(X_{t_1}), \cdots \sigma(X_{t_N}))$ of (5) from a single discrete data vector $(X_{t_0}, X_{t_1}, \cdots, X_{t_N})$. The second goal of the paper is to recover the symbolic function μ and σ from the above estimated vectors. Note that apriori we do not have information about the μ and σ function except for $\mu(X_0)$ and the fact that (5) has a unique (strong) solution (A sufficient condition for strong solution is (local) Lipschitz continuity of μ and σ).

Under the existence and uniqueness of solution of the SDE (5), the diffusion process of X_t given by (5) possesses the integral form

$$X_t = X_0 + \int_0^t \mu(X_s)ds + \int_0^t \sigma(X_s)dB_s^{\mathbb{P}},\tag{6}$$

where the stochastic integral is understood in the Itô sense. The equation (6) can be rewritten such that the stochastic integral is understood in the Stratonovich sense:

$$X_t = X_0 + \int_0^t \left(\mu(X_s) - \frac{1}{2} \sigma(X_s) \sigma'(X_s) \right) ds + \int_0^t \sigma(X_s) \circ dB_s^{\mathbb{P}}.$$
 (7)

The term $\frac{1}{2} \int_0^t \sigma(X_s) \sigma'(X_s) ds$ is known as the Itô-Stratnovich correction term or quadratic variation correction term corresponding to the SDE (6). If we set $\tilde{\mu}(X_s) := \mu(X_s) - \frac{1}{2}\sigma(X_s)\sigma'(X_s)$, then the SDE becomes

$$X_t = X_0 + \int_0^t \tilde{\mu}(X_s)ds + \int_0^t \sigma(X_s) \circ dB_s^{\mathbb{P}}.$$
 (8)

We will solve the problem in two-fold; firstly by estimating the diffusion vector and underlying risk-neutral Brownian noise. Secondly, by applying a series of approximations to simplify the SDE, and then using regression to identify the noise (underlying physical Brownian motion) and the drift vector simultaneously as a solution to the ODE. The detailed algorithm is provided in Section 3. Below is the list of assumptions we need to derive the algorithm.

- μ and σ are Lipschitz continuous.
- $\mu \in C^3(\mathbb{R})$ and $\sigma \in C^4(\mathbb{R})$.
- Assume the initial values of μ i.e. $\mu(X_0)$ is known (we do not need prior knowledge of $\sigma(X_0)$).
- Assume the \mathbb{P} Brownian motion starts at 0 i.e. $B_0^{\mathbb{P}} = 0$. Without this assumption, the algorithm still applies; however, we can only recover the increments of the noise vector rather than the noise vector itself.

We summarize the key steps behind the algorithm below.

Step 1: Firstly, by taking the quadratic variation of the original data process X_t , we can eliminate the drift μ and the randomness $B^{\mathbb{P}}$ from the system. This enables us to estimate the diffusion vector $(\sigma(X_{t_0}), \sigma(X_{t_1}), \cdots \sigma(X_{t_{N-1}}))$, of (5). We then use Girsanov's theorem to construct a measure \mathbb{Q} (often known as martingale /risk-neutral measure²) under which the drift in (5) disappears. i.e.

$$X_t = X_0 + \int_0^t -\frac{1}{2}\sigma(X_s)\sigma'(X_s)ds + \int_0^t \sigma(X_s) \circ dB_s^{\mathbb{Q}}.$$
 (9)

As a consequence, the risk-neutral Brownian noise (denoted as $B^{\mathbb{Q}}$) can be calculated at time points t_0, t_1, \dots, t_{N-1} using the data and the (estimated) diffusion vector.

By using a symbolic regression (based on a preset library), we then recover the underlying diffusion function $\sigma: \mathbb{R} \to \mathbb{R}$. This allows us to directly calculate the σ' vector in **Step 5** without using finite difference methods.

 $^{^1\}mathrm{We}$ use the notation $B^{\mathbb{P}}$ to stress the underlying probability measure

²This measure $\mathbb Q$ can be thought of as an artificial "lens" under which the data process X_t looks like fair games

- Step 2: For all $i \in \{0, \dots N-1\}$ we use a change of variable formula to rewrite $\sigma(X_{t_{i+1}})$ as an expansion around X_{t_i} . Replacing this approximation of σ in the (Stratonovich) integral form of SDE (9) and combining the like terms to represent the SDE in terms of weighted sums of the (Stratonovich) iterated integral (often identified as signatures) for the $B^{\mathbb{Q}}$ up to order two³, we identify the weights.
- Step 3: We approximate both the drift and diffusion coefficients $\mu(X_{t_{i+1}}), \sigma(X_{t_{i+1}})$ by a second-order Taylor expansion around (X_{t_i}) and replace the approximation into (8). This way we can represent the SDE (8) in terms of weighted sums of the (Stratonovich) iterated integral wrt the $B^{\mathbb{Q}}$ up to order two, and we identify the weights.
- Step 4: We now apply the Girsanov theorem to transform our approximated SDE in **Step 3** into an approximated SDE written as a sum of weighted (Stratonovich) iterated integral with respect to the martingale Brownian motion $B^{\mathbb{Q}}$ up to order two.
- Step 5: For each time interval $[t_i^n, t_{i+1}^n)$ by comparing the weights from **Step 2** and **Step 4**, we write μ as a solution of ODE where the coefficients of the ODE are written using σ , σ' and the weights from **Step 2**.
- Step 6: We use a regression method to solve the weights from **Step 3** to identify the coefficients of the ODE in **Step 5**. Finally, we use an ODE solver on the time grid (t_1, \dots, t_N) to identify the drift vector $(\mu(X_{t_0}), \mu_(X_{t_1}), \dots \mu(X_{t_N}))$ and recover the increments of the physical Brownian motion $\{\Delta B_{t_i}^{\mathbb{P}} := B_{t_i+1}^{\mathbb{P}} B_{t_i}^{\mathbb{P}}\}_{i=1}^{N-1}$.
- Step 7: We propose Stochastic Sparse Identification of Stochastic Differential Equation (SSISDE) to recover the exact symbolic form of the SDE that

$$dX_t = \mu(X_t)dt + \sigma(X_t)dB_t^{\mathbb{P}}. (10)$$

We introduced a stochastic symbolic regression problem inspired by SINDy, which allowed us to obtain the precise functional form of the SDE by optimizing the following target

$$\arg\min_{\Xi_{\sigma},\Xi_{\mu}} \sum_{i=i}^{N} ||\Delta X_{t_i} - \Theta(X_{t_i})\Xi_{\mu}\Delta t_i - \Theta(X_{t_i})\Xi_{\sigma}\Delta B_{t_i}^{\mathbb{P}}||_2^2 + \mathcal{R}_{\alpha,\rho}(\Xi_{\mu},\Xi_{\sigma}), \tag{11}$$

where $\Theta(X_{t_i})$ is a library of functions (pre-)specified by the users, which commonly includes polynomials and Fourier functions. This concludes our algorithm to identify the stochastic governing equation from noisy, stochastic, and single-shot time-series observations.

3 Main Results

In this section, we introduce the main algorithm. The key idea is to formulate the estimator of the drift function as the solution of an ODE, which in turn enables the recovery of the underlying physical Brownian motion $B^{\mathbb{P}}$ given one single trajectory observation of the state process X_t on a finite time interval [0,T].

Step 1: recovering Q-Brownian motion. Recast the Itô SDE (5) with stating time s (may or may not be 0) and terminal time t > s below,

$$X_t = X_s + \int_s^t \mu(X_u) du + \int_s^t \sigma(X_u) dB_u^{\mathbb{P}}.$$
 (12)

By applying Girsanov's theorem, the above SDE can be represented as a martingale with respect to the \mathbb{Q} -Brownian motion $B^{\mathbb{Q}}$, which has the following form

$$X_t = X_s + \int_{-t}^{t} \sigma(X_u) dB_u^{\mathbb{Q}} \tag{13}$$

where $B^{\mathbb{Q}}$ is the Brownian motion under the martingale measure \mathbb{Q} , which is often referred to risk-neutral measure in finance Harrison and Pliska (1981), following the dynamic

$$\forall u \in [s, t); \quad dB_u^{\mathbb{Q}} = dB_u^{\mathbb{P}} + \frac{\mu(X_u)}{\sigma(X_u)} dt, \tag{14}$$

By definition, the underlying limiting quadratic variation of process X along a given sequence of time-grid $\pi:=\{\pi^N\}_{N=0}^{\infty}:=\{0=t_0^N< t_1^N\cdots< t_i^N<\cdots< t_{\#(\pi^N)}^N=t\}_{N=0}^{\infty}$ with vanishing mesh (i.e. $|t_{i+1}^N-t_i^N|\xrightarrow{N\to\infty}$ 0), denoted by $[X]_{\pi,t}:=\lim_{n\to\infty}\sum_{\pi^n\cap[0,t]}(X(t_{i+1}^n)-X(t_i^n))^2$, has the following form

$$d[X]_{\pi,t} = (\sigma(X_t))^2 dt. \tag{15}$$

³By order two we mean the error terms are of order $|t_{i+1}^n - t_i^n|^{2-\epsilon}$ for any given $\epsilon > 0$.

By using the high frequency estimate of quadratic variation along the time-grid π^M for a given M large enough (i.e $[X]_{\pi^M,t} := \sum_{\pi^M \cap [0,t]} (X(t_{i+1}^M) - X(t_i^M))^2$), we first obtain an estimate of σ as follows.

$$(\sigma(X_t))^2 \approx \frac{1}{\delta} \sum_{\pi^M \cap [t, t+\delta]} (X(t_{i+1}^M) - X(t_i^M))^2$$
 (16)

Note that in order to approximate the diffusion vector $(\sigma(X_{t_0}), \sigma(X_{t_1}), \cdots, \sigma(X_{t_{N-1}}))$ one need to have observation of the underlying process X along a finer grid, i.e. $\sigma(X_{t_i})$ is calculated by talking sum square difference of L many observation of X between t_i and t_{i+1} . Once the σ vector has been identified, we can then construct the \mathbb{Q} -Brownian motion increment on any interval $[t, t + \delta]$, for $\delta > 0$,

$$B_{t+\delta}^{\mathbb{Q}} - B_t^{\mathbb{Q}} = \int_t^{t+\delta} \frac{dX_s}{\sigma(X_s)} \approx \frac{\sqrt{\delta}(X(t+\delta) - x(t))}{\sqrt{\sum_{\pi^M \cap [t, t+\delta]} (X(t_{i+1}^M) - X(t_i^M))^2}}.$$
 (17)

leaning σ function from the vector $(\sigma(X_{t_0}), \sigma(X_{t_1}), \dots, \sigma(X_{t_{N-1}}))$ By considering the input-output pairs $\{(X_{t_i}, \sigma(X_{t_i}))\}$, we build a library $\Theta(X_{t_i})$ and rewrite (generalized) SINDy into a symbolic regression form as follows.

$$\Xi_{\sigma}^{*} = \arg\min_{\Xi_{\sigma}} \sum_{i=0}^{N-1} ||\sigma(X_{t_{i}}) - \Theta(X_{t_{i}})\Xi_{\sigma}|| + ||\Xi_{\sigma}||_{0},$$
(18)

where the first loss is to fit the model (i.e., the function σ), and the second term is referred to as sparsity regularization. This optimization problem can be solved using a sequential thresholding least-squares algorithm in SINDy. Since the coefficient of Ξ_{σ} is sparse, this optimization problem effectively identifies the symbolic functional form of the $\sigma(X_{t_i})$ (e.g., for the BS equation $\sigma(X_{t_i}) = \sigma X_{t_i}$). Note that from (16) we can not recover the terminal value $\sigma(X_{t_N})$, but once we estimate the σ function from (18) one can estimate $\sigma(X_{t_N})$, recovering the entire diffusion vector $(\sigma(X_{t_0}), \sigma(X_{t_1}), \cdots \sigma(X_{t_N}))$.

Step 2: constructing estimator for X_t via Stratonovich SDE. For the Itô SDE (13), the corresponding Stratonovich SDE has the following form,

$$X_t = X_s + \int_s^t -\frac{1}{2}\sigma(X_u)\sigma'(X_u)du + \int_s^t \sigma(X_u) \circ dB_u^{\mathbb{Q}}$$

:= $X_s + \int_s^t A_0(X_u)du + \int_s^t \sigma(X_u) \circ dB_u^{\mathbb{Q}},$ (19)

where we denote $A_0(X_t) = -\frac{1}{2}\sigma(X_t)\sigma'(X_t)$, which is commonly known as the Itô-Stratonovich correction term. For the Stratonovich SDE (19), applying the (Stratonovich) change of variable formula (i.e. $f(X_u) = f(X_s) + \int_s^u f'(X_r) \circ dX_r$) for the A_0 and σ functions around the initial point X_s , we get the following expansion. Under some nominal Hölder assumptions on the underlying process X, this approximation error is of order $|t|^{3/2}$ (i.e. $|t_{i+1} - t_i|^{\frac{3}{2}}$ on each time grid $[t_i, t_{i+1})$).

$$X_t = X_s + A_0(X_s) \int_s^t du + \int_s^t \int_s^u A_0'(X_r) \circ dX_r du + \sigma(X_s) \int_s^t \circ dB_u^{\mathbb{Q}} + \int_s^t \int_s^u \sigma'(X_r) \circ dX_r \circ dB_u^{\mathbb{Q}}.$$

Plugging the differential from of the dynamic (19) into the above expansion, applying the change of variable iteratively, and finally approximating $\sigma(X_u)$ for all $u \in [t_i, t_{i+1})$ by $\sigma(X_{t_i})$ we get the following second-order expansion⁴ of the process X_t in the Stratonovich form,

$$X_{t} = X_{s} + \psi_{1}^{s,t} \int_{s}^{t} du + \psi_{2}^{s,t} \int_{s}^{t} \circ dB_{u} + \psi_{12}^{s,t} \int_{s}^{t} \int_{s}^{u} dr \circ dB_{u}^{\mathbb{Q}}$$

$$+ \psi_{21}^{s,t} \int_{s}^{t} \int_{s}^{u} \circ dB_{r}^{\mathbb{Q}} du + \psi_{22}^{s,t} \int_{s}^{t} \int_{s}^{u} \circ dB_{r}^{\mathbb{Q}} \circ dB_{u}^{\mathbb{Q}} + \psi_{222}^{s,t} \int_{s}^{t} \int_{s}^{u} \int_{s}^{r} \circ dB_{v}^{\mathbb{Q}} \circ dB_{r}^{\mathbb{Q}} \circ dB_{u}^{\mathbb{Q}} + \varepsilon^{\Psi_{2}},$$

$$(20)$$

where we denote ε^{Ψ_2} as the error for the higher-order Taylor expansion terms (see, e.g., Kloeden and Platen (1992)). The detailed derivation is provided in subsection 3.1. In the following, we will call the set $\Psi_2^{s,t}$ the second-order estimator of the diffusion process for the interval [s,t], and denote it as

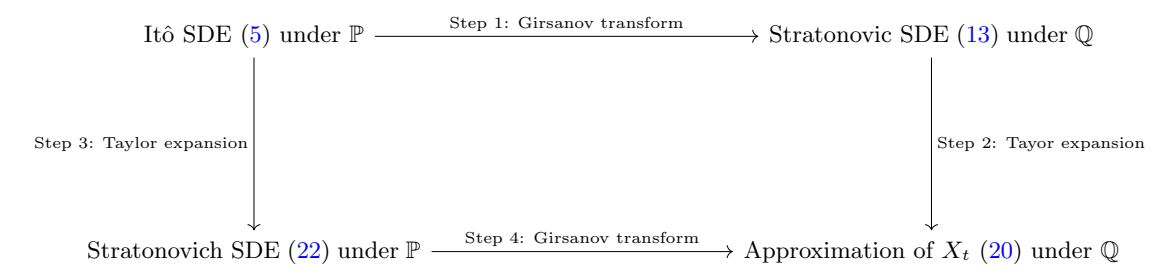
$$\Psi_2^{s,t} := \{ \psi_1^{s,t}, \psi_2^{s,t}, \psi_{12}^{s,t}, \psi_{21}^{s,t}, \psi_{22}^{s,t}, \psi_{222}^{s,t} \}. \tag{21}$$

Note that the estimate of the set $\Psi_2^{s,t}$ does depend on the full data on the interval [s,t], whereas theoretically the set $\Psi_2^{s,t}$ only depends on observations at time s. Essentially, the set $\Psi_2^{s,t}$ is a collection of different

⁴by the second order we mean the error term is of the order $O(|t-s|^{2-\delta})$ for any $\delta > 0$.

combinations of σ and all its derivatives evaluated at the initial value X_s . For example, $\psi_1^{s,t} = A_0(X_s)$ and $\psi_2^{s,t} = \sigma(X_s)$. Finally, we use the estimated \mathbb{Q} -Brownian motion $B^{\mathbb{Q}}$ from **Step 1** to find estimators in $\Psi_2^{s,t}$ for the second order model (20).

Next, instead of applying the Girsanov transformation first as done in **Step 1**, we will apply the Taylor expansion first directly for the Stratonovich SDE under Wiener measure \mathbb{P} in **Step 3**, and then apply the Girsanov transformation in the last step (**Step 4**) to construct the estimator of the function μ . The explicit algorithm is demonstrated in the following diagram.



Step 3: Taylor expansion of Stratonovich SDE under Wiener measure \mathbb{P} . Recall the Stratonovich SDE (8) with a (deterministic) starting time s (not necessarily 0) with respect to the physical measure \mathbb{P} :

$$X_t = X_s + \int_s^t \tilde{\mu}(X_u) du + \int_s^t \sigma(X_u) \circ dB_u^{\mathbb{P}}.$$

Applying stochastic Taylor expansion on $\tilde{\mu}$ and σ around the initial observation X_s , and truncating the Taylor expansion at level 2 (see e.g. Kloeden and Platen (1992)), we have the following (up to second order derivatives of $\tilde{\mu}$ and σ) Taylor expansion approximation of X_t under Wiener measure \mathbb{P} ,

$$X_{t} = X_{s} + \tilde{\mu}(X_{s}) \int_{s}^{t} du + \sigma(X_{s}) \int_{s}^{t} \circ dB_{u}^{\mathbb{P}} + \tilde{\mu}'(X_{s})\tilde{\mu}(X_{s}) \int_{s}^{t} \int_{s}^{u} dr du + \tilde{\mu}'(X_{s})\sigma(X_{s}) \int_{s}^{t} \int_{s}^{u} \circ dB_{r}^{\mathbb{P}} du$$

$$+ \sigma'(X_{s})\tilde{\mu}(X_{s}) \int_{s}^{t} \int_{s}^{u} dr \circ dB_{u}^{\mathbb{P}} + \sigma'(X_{s})\sigma(X_{s}) \int_{s}^{t} \int_{s}^{u} \circ dB_{r}^{\mathbb{P}} \circ dB_{u}^{\mathbb{P}}$$

$$+ ((\tilde{\mu}'(X_{s}))^{2}\tilde{\mu}(X_{s}) + \tilde{\mu}''(X_{s})(\tilde{\mu}(X_{s}))^{2}) \int_{s}^{t} \int_{s}^{u} \int_{s}^{r} dv dr du$$

$$+ ((\tilde{\mu}'(X_{s}))^{2}\sigma(X_{s}) + \tilde{\mu}''(X_{s})\tilde{\mu}(X_{s})\sigma(X_{s})) \int_{s}^{t} \int_{s}^{u} \int_{s}^{r} odB_{v}^{\mathbb{P}} dr du$$

$$+ (\tilde{\mu}'(X_{s})\sigma'(X_{s})\tilde{\mu}(X_{s}) + \tilde{\mu}''(X_{s})(\tilde{\mu}(X_{s}))^{2}) \int_{s}^{t} \int_{s}^{u} \int_{s}^{r} dv \circ dB_{r}^{\mathbb{P}} du$$

$$+ (\tilde{\mu}'(X_{s})\sigma'(X_{s})\sigma(X_{s}) + \tilde{\mu}''(X_{s})(\sigma(X_{s}))^{2}) \int_{s}^{t} \int_{s}^{u} \int_{s}^{r} odB_{v}^{\mathbb{P}} \circ dB_{v}^{\mathbb{P}} du$$

$$+ (\tilde{\mu}'(X_{s})\sigma'(X_{s})\sigma(X_{s}) + \tilde{\mu}''(X_{s})(\sigma(X_{s}))^{2}) \int_{s}^{t} \int_{s}^{u} \int_{s}^{r} odB_{v}^{\mathbb{P}} \circ dB_{v}^{\mathbb{P}} dv \circ dB_{u}^{\mathbb{P}}$$

$$+ ((\sigma'(X_{s}))^{2}\tilde{\mu}(X_{s}) + \sigma''(X_{s})\sigma(X_{s})\tilde{\mu}(X_{s})) \int_{s}^{t} \int_{s}^{u} \int_{s}^{r} odB_{v}^{\mathbb{P}} \circ dB_{v}^{\mathbb{P}} \circ dB_{u}^{\mathbb{P}}$$

$$+ ((\sigma'(X_{s}))^{2}\sigma(X_{s}) + \sigma''(X_{s})(\sigma(X_{s}))^{2}) \int_{s}^{t} \int_{s}^{u} \int_{s}^{r} odB_{v}^{\mathbb{P}} \circ dB_{v}^{\mathbb{P}} \circ dB_{u}^{\mathbb{P}} + \varepsilon^{\tilde{\mu},\sigma}, \tag{22}$$

where $\varepsilon^{\tilde{\mu},\sigma}$ denotes the higher order approximation error term. The proof of this claim is postponed to the following subsection 3.2, along with the discussion of the error term $\varepsilon^{\tilde{\mu},\sigma}$.

Step 4: Girsanov transformation. Applying the Girsanov theorem, substituting for all $r \in [s,t)$; $dB_r^{\mathbb{P}} = dB_r^{\mathbb{Q}} - \frac{\mu(X_r)}{\sigma(X_r)}dt$ into the Stratonovich SDE approximation (22), we have the following second order approximation expansion of X_t

$$X_t = X_s - \frac{1}{2}\sigma(X_s)\sigma'(X_s) \int_s^t du + \sigma(X_s) \int_s^t \circ dB_u^{\mathbb{Q}}$$
$$+ \left(\mu'(X_s)\sigma(X_s) - \mu(X_s)\sigma'(X_s) - \frac{1}{2}\sigma(X_s)\sigma'(X_s)^2 - \frac{1}{2}\sigma(X_s)^2\sigma''(X_s)\right) \int_s^t \int_s^u \circ dB_r^{\mathbb{Q}} du$$

$$-\frac{1}{2}\sigma(X_s)\sigma'(X_s)^2 \int_s^t \int_s^r du \circ dB_r^{\mathbb{Q}} + \sigma'(X_s)\sigma(X_s) \int_s^t \int_s^u \circ dB_r^{\mathbb{Q}} \circ dB_u^{\mathbb{Q}}$$
$$+ \left((\sigma'(X_s))^2 \sigma(X_s) + \sigma''(X_s)(\sigma(X_s))^2 \right) \int_s^t \int_s^u \int_s^r \circ dB_v^{\mathbb{Q}} \circ dB_r^{\mathbb{Q}} \circ dB_u^{\mathbb{Q}} + \varepsilon^{\tilde{\mu},\sigma} + \varepsilon^{\mu/\sigma}. \tag{23}$$

where the error term $\varepsilon^{\tilde{\mu},\sigma}$ is due to (22), and the error term $\varepsilon^{\mu/\sigma}$ is due to the approximation of $\frac{\mu(X_u)}{\sigma(X_u)}$ by the initial condition $\frac{\mu(X_s)}{\sigma(X_s)}$ for $u \in [s,t]$. We want to remark that only when |t-s| is small the error term $\varepsilon^{\mu/\sigma}$ can be controlled and is of order $|t-s|^{2-\epsilon}$ for |t-s| small and any $\epsilon > 0$, not for general s,t. In particular, following the Taylor expansion Azencott (2006) and the Castell estimates Castell (1993), the error term $\varepsilon^{\tilde{\mu},\sigma} + \varepsilon^{\mu/\sigma}$ follows a Gaussian tail estimate. The expected error (under $\mathbb{E}^{\mathbb{Q}}$) can be found in Lyons and Victoir (2004). The proof of this claim is postponed to Subsection 3.3.

Step 5: constructing estimator of μ . In this step we recursively calculate the drift vector $(\mu(X_{t_1}), \mu(X_{t_2}), \dots \mu(X_{t_N}))$ under the assumption of know initial value $\mu(X_{t_0})$ is known. By comparing the coefficients of same iterated integrals of (20) from **Step 2** and (23) from **Step 4** on the interval $[t_0, t_1)$ and under the assumption of know initial value $\mu(X_{t_0})$ we calculate the drift $\mu(X_{t_1})$, than recursively calculate all the other drift terms. Under the assumption that σ is continuous, it is enough for short time uniqueness of ODE for the drift function μ in the interval $[t_i, t_{i+1})$ for $|t_{i+1} - t_i| << 1$, and hence in the interval $[t_i, t_{i+1})$ the drift function can be written as the (unique) solution of the following ODE with given initial value $\mu(x_{t_i})$ (which is estimated from the previous step)

$$\mu'(x) = a(x)\mu(x) + b(x),$$
 (24)

where $a(x) = \frac{\sigma'(x)}{\sigma(x)}$ and $b(x) = \frac{2\psi_{21}^{[t_i, t_{i+1}]} + \sigma(x)\sigma'(x)^2 + \sigma(x)^2\sigma''(x)}{2\sigma(x)}$, and $\psi_{21}^{[t_i, t_{i+1}]}$ is defined in (20) from **Step 2** on the interal $[t_i, t_{i+1}]$. Note that we can identify the function σ and $a\sigma'$ from **Step 1**. The proof is postponed to Subsection 3.4.

Step 6: estimating the noise with \mathbb{P} -Brownian motion. By applying regression methods to find the estimator $\psi_{12}^{[t_i,t_{i+1})}$ recursively using the model constructed from the martingale Brownian motion $B^{\mathbb{Q}}$. Applying Step 1-5 to the single trajectory observation of the states $\{X_{t_i}\}_{i=1}^N$, we find the second order estimator for the drift vector μ at the time grid t_1, \dots, t_N as the solution of ODE (24). Then, applying the change of measure (14) to recover the noise increment vectors $(\Delta B_{t_0}^{\mathbb{P}}, \Delta B_{t_2}^{\mathbb{P}}, \dots, \Delta B_{t_{N-1}}^{\mathbb{P}})$ by using the following discretization scheme,

$$\Delta B_{t_i}^{\mathbb{Q}} = \Delta B_{t_i}^{\mathbb{P}} + \frac{\mu(X_{t_i})}{\sigma(X_{t_i})} \Delta t_i, \quad \text{for} \quad i = 1, \dots, N,$$
(25)

where we use the convection $\Delta B_{t_i}^{\mathbb{P}} = B_{t_{i+1}}^{\mathbb{P}} - B_{t_i}^{\mathbb{P}}$ (similarly for $B^{\mathbb{Q}}$ and t).

Step 7: SSISDE to recover drift and diffusion function. We now present the Stochastic Sparse Identification of Stochastic Differential Equation (SSISDE) algorithm, which is able to precisely identify the form of the governing SDE (5)

$$dX_t = \mu(X_t)dt + \sigma(X_t)dB_t^{\mathbb{P}}$$

If X_t and the noise $B_t^{\mathbb{P}}$ can be observed along the time grid $t_1 < \cdots < t_N$, this can be viewed as a symbolic regression problem that

$$dX_t = \Theta_{\mu}(X_t)\Xi_{\mu}dt + \Theta_{\sigma}(X_t)\Xi_{\sigma}dB_t^{\mathbb{P}}, \tag{26}$$

which is motivated from the the sparse identification of nonlinear dynamics (SINDy) Brunton et al. (2016). Following the idea of SINDY, According to **Step 6**, we have constructing the original noise increment $\{\Delta B_{t_i}^{\mathbb{P}}\}_{i=0}^{N-1}$ from observation data $\{X_{t_i}\}_{i=0}^{N}$. We construct symbolic regression for the following identity

$$\Delta X_{t_i} = \Theta_{\mu}(X_{t_i}) \Xi_{\mu} \Delta t_i + \Theta_{\sigma}(X_{t_i}) \Xi_{\sigma} \Delta B_{t_i}^{\mathbb{P}}, \tag{27}$$

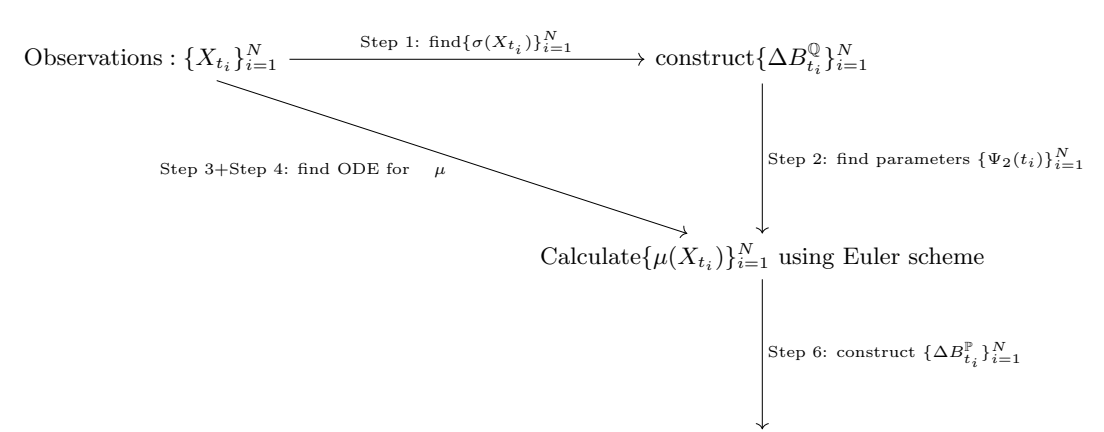
for $i=0,\dots,N-1$. We denote Ξ_{σ} (and Ξ_{μ} respectively) as the unknown sparse matrix corresponding to function σ (and μ respectively). Similarly, we denote $\Theta_{\sigma}(\cdot)$ and $\Theta_{\mu}(\cdot)$ as the candidate models for σ and μ . We thus propose the following *Stochastic Sparse Identification of Stochastic Differential Equation* (SSISDE) algorithm, which can be written as a stochastic symbolic regression problem,

$$\arg\min_{\Xi_{\sigma},\Xi_{\mu}} \sum_{i=0}^{N-1} ||\Delta X_{t_i} - \Theta_{\mu}(X_{t_i})\Xi_{\mu}\Delta t_i - \Theta_{\sigma}(X_{t_i})\Xi_{\sigma}\Delta B_{t_i}^{\mathbb{P}}||_2^2 + \mathcal{R}_{\alpha,\rho}(\Xi_{\mu},\Xi_{\sigma}), \tag{28}$$

where the first term is the residual L_2 -norm, and the second is a sparsity-inducing regularizer.

Remark 3.1. The Stochastic Sparse Identification of Stochastic Differential Equation (SSISDE) (28) only takes input data ΔX_{t_i} and the estimated noise $\Delta B_{t_i}^{\mathbb{P}}$, which is different from the SINDy form (18) in **Step 5**. In the end, one can compare the estimated symbolic forms for the function σ . In general, we only use (18) in **Step 5** to construct the estimate of the drift vector $\mu(X_{t_i})$ and the desired noise $\Delta B_{t_i}^{\mathbb{P}}$.

The main algorithm is described below.



Step 7: apply SSISDE to identify the two functions μ, σ .

3.1 Proof of Step 2.

Proof. Recall that

$$X_t = X_s + A_0(X_s) \int_s^t du + \int_s^t \int_s^u A_0'(X_r) \circ dX_r du + \sigma(X_s) \int_s^t \circ dB_u^{\mathbb{Q}} + \int_s^t \int_s^u \sigma'(X_r) \circ dX_r \circ dB_u^{\mathbb{Q}}.$$

Plugging in the dynamics of dX_r (19) and applying the Taylor expansion at the starting point X_s , we get

$$X_{t} = X_{s} + A_{0}(X_{s}) \int_{s}^{t} du + \int_{s}^{t} \int_{s}^{u} A'_{0}(X_{r})(A_{0}(X_{r})dr + \sigma(X_{r}) \circ dB_{r}^{\mathbb{Q}})du + \sigma(X_{s}) \int_{s}^{t} \circ dB_{u}^{\mathbb{Q}}$$

$$+ \int_{s}^{t} \int_{s}^{u} \sigma'(X_{r})(A_{0}(X_{r})dr + \sigma(X_{r}) \circ dB_{r}^{\mathbb{Q}}) \circ dB_{u}^{\mathbb{Q}}$$

$$= X_{s} + A_{0}(X_{s}) \int_{s}^{t} du + A'_{0}(X_{s})A_{0}(X_{s}) \int_{s}^{t} \int_{s}^{u} dr du + A_{0}(X_{s}) \int_{s}^{t} du + A'_{0}(X_{s})\sigma(X_{s}) \int_{s}^{t} \int_{s}^{u} \circ dB_{r}^{\mathbb{Q}} du$$

$$+ \sigma(X_{s}) \int_{s}^{t} \circ dB_{u}^{\mathbb{Q}} + \sigma'(X_{s})A_{0}(X_{s}) \int_{s}^{t} \int_{s}^{u} dr \circ dB_{u}^{\mathbb{Q}} + \sigma'(X_{s})\sigma(X_{s}) \int_{s}^{t} \int_{s}^{u} \circ dB_{r}^{\mathbb{Q}} \circ dB_{u}^{\mathbb{Q}}$$

$$+ \int_{s}^{t} \int_{s}^{u} \int_{s}^{r} (A''_{0}(X_{v})A_{0}(X_{v}) + A'_{0}(X_{v})A'_{0}(X_{v})) \circ dX_{v} dr \circ dB_{u}^{\mathbb{Q}} du$$

$$+ \int_{s}^{t} \int_{s}^{u} \int_{s}^{r} (\sigma''(X_{v})A_{0}(X_{v}) + \sigma'(X_{v})A'_{0}(X_{v})) \circ dX_{v} dr \circ dB_{u}^{\mathbb{Q}}$$

$$+ \int_{s}^{t} \int_{s}^{u} \int_{s}^{r} (\sigma''(X_{v})A_{0}(X_{v}) + \sigma'(X_{v})A'_{0}(X_{v})) \circ dX_{v} dr \circ dB_{u}^{\mathbb{Q}}$$

$$+ \int_{s}^{t} \int_{s}^{u} \int_{s}^{r} (\sigma''(X_{v})A_{0}(X_{v}) + \sigma'(X_{v})A'_{0}(X_{v})) \circ dX_{v} dr \circ dB_{u}^{\mathbb{Q}}$$

$$+ \int_{s}^{t} \int_{s}^{u} \int_{s}^{r} (\sigma''(X_{v})A_{0}(X_{v}) + \sigma'(X_{v})A'_{0}(X_{v})) \circ dX_{v} dr \circ dB_{u}^{\mathbb{Q}}$$

We collect higher order terms (i.e., with order equal or higher than $|t-s|^{2-\varepsilon}$, for any $\varepsilon > 0$, when |t-s| is small) and denote them as the error term ε^{Ψ_2} . The leading term of $\int_s^t \int_s^u \int_s^r (\sigma''(X_v)\sigma(X_v) + \sigma'(X_v)\sigma'(X_v)) \circ dX_v \circ dB_v^{\mathbb{Q}} \circ dB_u^{\mathbb{Q}}$ will contribute one more $|t-s|^{3/2-\varepsilon}$ term, which has the following form,

$$\left(\sigma''(X_s)\sigma(X_s) + \sigma'(X_s)\sigma'(X_s)\right)\sigma(X_s)\int_s^t\int_s^u\int_s^r \circ dB_v^{\mathbb{Q}} \circ dB_r^{\mathbb{Q}} \circ dB_u^{\mathbb{Q}},$$

together with higher-order error terms. By collecting all the second-order iterated integrals, where the integral against Brownian motion has order $\frac{1}{2} - \varepsilon$, we end up with

$$X_t = X_s + \psi_1^{s,t} \int_s^t du + \psi_2^{s,t} \int_s^t dB_u + \psi_{12}^{s,t} \int_s^t \int_s^u dr \circ dB_u^{\mathbb{Q}}$$

$$+ \ \psi_{21}^{s,t} \int_{t}^{t} \int_{u}^{u} \circ dB_{r}^{\mathbb{Q}} du + \psi_{22}^{s,t} \int_{t}^{t} \int_{u}^{u} \circ dB_{r}^{\mathbb{Q}} \circ dB_{u}^{\mathbb{Q}} + \psi_{222}^{s,t} \int_{t}^{t} \int_{u}^{u} \int_{r}^{r} \circ dB_{v}^{\mathbb{Q}} \circ dB_{r}^{\mathbb{Q}} \circ dB_{u}^{\mathbb{Q}} + \varepsilon^{\Psi_{2}},$$

where we denote $\Psi_2^{s,t} := \{\psi_1^{s,t}, \psi_2^{s,t}, \psi_{12}^{s,t}, \psi_{21}^{s,t}, \psi_{22}^{s,t}, \psi_{222}^{s,t}\}$ as the coefficients of the second order expansion of X_t , and $\varepsilon^{\Psi_2} (\approx |t-s|^{2-\varepsilon})$ as the error term for the second order expansion. The proof is thus completed. \square

3.2 Proof of Step 3.

Proof: Applying stochastic Taylor expansion on $\tilde{\mu}$ and σ around X_s , and truncating the Taylor expansion at level 2, we have the following approximation of $\tilde{\mu}$ and σ ,

$$\tilde{\mu}(X_u) = \tilde{\mu}(X_s) + \tilde{\mu}'(X_s) \int_s^u \circ dX_r + \tilde{\mu}''(X_s) \int_s^u \int_s^r \circ dX_v \circ dX_r + \underbrace{\int_s^u \int_s^r \int_s^v \tilde{\mu}'''(\xi_\tau) \circ dX_\tau \circ dX_v \circ dX_r}_{\varepsilon \tilde{\mu}}$$

$$(30)$$

$$\sigma(X_u) = \sigma(X_s) + \sigma'(X_s) \int_s^u \circ dX_r + \sigma''(X_s) \int_s^u \int_s^r \circ dX_v \circ dX_r + \underbrace{\int_s^u \int_s^r \int_s^v \tilde{\mu}'''(\eta_\tau) \circ dX_\tau \circ dX_v \circ dX_r}_{\varepsilon \sigma}$$

$$(31)$$

Where we denote $\varepsilon^{\tilde{\mu}}$ and ε^{σ} as the higher order approximation error wrt the second order expansion. Under some nominal Hölder assumptions on the underlying process X and smoothness of the functions $\tilde{\mu}$ and σ , these approximation errors of (30) and (31) are of order $|t_{i+1} - t_i|^{\frac{3}{2} - \varepsilon}$ on each time grid $[t_i, t_{i+1}]$. For clarity, we highlight the substitution of the expansion into the dynamics in blue. Substituting the second-order Taylor expansions (30) and (31) into (8) gives

$$X_{t} = X_{s} + \int_{s}^{t} \left(\tilde{\mu}(X_{s}) + \tilde{\mu}'(X_{s}) \int_{s}^{u} \circ dX_{r} + \tilde{\mu}''(X_{s}) \int_{s}^{u} \int_{s}^{r} \circ dX_{v} \circ dX_{r} + \varepsilon^{\tilde{\mu}} \right) du$$
$$+ \int_{s}^{t} \left(\sigma(X_{s}) + \sigma'(X_{s}) \int_{s}^{u} \circ dX_{r} + \sigma''(X_{s}) \int_{s}^{u} \int_{s}^{r} \circ dX_{v} \circ dX_{r} + \varepsilon^{\sigma} \right) \circ dB_{u}^{\mathbb{P}}.$$

Plugging in dynamic (8) for dX_t in the above expansion, we get

$$\begin{split} X_t &= X_s + \tilde{\mu}(X_s) \int_s^t du + \sigma(X_s) \int_s^t \circ dB_u^{\mathbb{P}} + \tilde{\mu}'(X_s) \int_s^t \int_s^u \left(\tilde{\mu}(X_r) dr + \sigma(X_r) \circ dB_r^{\mathbb{P}} \right) du \\ &+ \tilde{\mu}''(X_s) \int_s^t \int_s^u \int_s^r \left(\tilde{\mu}(X_v) dv + \sigma(X_v) \circ dB_v^{\mathbb{P}} \right) \left(\tilde{\mu}(X_r) dr + \sigma(X_r) \circ dB_r^{\mathbb{P}} \right) du \\ &+ \sigma'(X_s) \int_s^t \int_s^u \left(\tilde{\mu}(X_r) dr + \sigma(X_r) \circ dB_r^{\mathbb{P}} \right) \circ dB_u^{\mathbb{P}} \\ &+ \sigma''(X_s) \int_s^t \int_s^u \int_s^r \left(\tilde{\mu}(X_v) dv + \sigma(X_v) \circ dB_v^{\mathbb{P}} \right) \left(\tilde{\mu}(X_r) dr + \sigma(X_r) \circ dB_r^{\mathbb{P}} \right) \circ dB_u^{\mathbb{P}} \\ &+ \varepsilon^{\tilde{\mu}} \int_s^t ds + \varepsilon^{\sigma} \int_s^t \circ dB_u^{\mathbb{P}} \\ &= X_s + \tilde{\mu}(X_s) \int_s^t du + \sigma(X_s) \int_s^t \circ dB_u^{\mathbb{P}} + \tilde{\mu}'(X_s) \int_s^t \int_s^u \tilde{\mu}(X_r) dr du + \tilde{\mu}'(X_s) \int_s^t \int_s^u \sigma(X_r) \circ dB_r^{\mathbb{P}} du \\ &+ \sigma'(X_s) \int_s^t \int_s^u \tilde{\mu}(X_r) dr \circ dB_u^{\mathbb{P}} + \sigma'(X_s) \int_s^t \int_s^u \sigma(X_r) \circ dB_r^{\mathbb{P}} \circ dB_u^{\mathbb{P}} \\ &+ \tilde{\mu}''(X_s) \int_s^t \int_s^u \int_s^r \left(\tilde{\mu}(X_v) dv + \sigma(X_v) \circ dB_v^{\mathbb{P}} \right) \left(\tilde{\mu}(X_r) dr + \sigma(X_r) \circ dB_r^{\mathbb{P}} \right) du \\ &+ \sigma''(X_s) \int_s^t \int_s^u \int_s^r \left(\tilde{\mu}(X_v) dv + \sigma(X_v) \circ dB_v^{\mathbb{P}} \right) \left(\tilde{\mu}(X_r) dr + \sigma(X_r) \circ dB_r^{\mathbb{P}} \right) \circ dB_u^{\mathbb{P}} \\ &+ \varepsilon^{\tilde{\mu}} \int_s^t du + \varepsilon^{\sigma} \int_s^t \circ dB_u^{\mathbb{P}} \end{split}$$

For the double integral in the above expansion, apply first-order Taylor expansion for $\tilde{\mu}(X_r)$ and $\sigma(X_r)$ at X_s and plug in the dynamic for dX_t again, we further get

$$X_t = X_s + \tilde{\mu}(X_s) \int_s^t du + \sigma(X_s) \int_s^t \circ dB_u^{\mathbb{P}} + \tilde{\mu}'(X_s) \tilde{\mu}(X_s) \int_s^t \int_s^u dr du + \tilde{\mu}'(X_s) \sigma(X_s) \int_s^t \int_s^u \circ dB_r^{\mathbb{P}} du$$

Finally, replacing $\tilde{\mu}$ and σ with their Taylor expansion around X_s and combining the like terms up to triple integrals, gives the following expansion

$$\begin{split} X_t &= X_s + \tilde{\mu}(X_s) \int_s^t du + \sigma(X_s) \int_s^t \circ dB_u^{\mathbb{P}} + \tilde{\mu}'(X_s) \tilde{\mu}(X_s) \int_s^t \int_s^u dr du + \tilde{\mu}'(X_s) \sigma(X_s) \int_s^t \int_s^u \circ dB_r^{\mathbb{P}} du \\ &+ \sigma'(X_s) \tilde{\mu}(X_s) \int_s^t \int_s^u dr \circ dB_u^{\mathbb{P}} + \sigma'(X_s) \sigma(X_s) \int_s^t \int_s^u \circ dB_r^{\mathbb{P}} \circ dB_u^{\mathbb{P}} \\ &+ \left((\tilde{\mu}'(X_s))^2 \tilde{\mu}(X_s) + \tilde{\mu}''(X_s) (\tilde{\mu}(X_s))^2 \right) \int_s^t \int_s^u \int_s^r dv dr du \\ &+ \left((\tilde{\mu}'(X_s))^2 \sigma(X_s) + \tilde{\mu}''(X_s) \tilde{\mu}(X_s) \sigma(X_s) \right) \int_s^t \int_s^u \int_s^r \circ dB_v^{\mathbb{P}} dr du \\ &+ \left(\tilde{\mu}'(X_s) \sigma'(X_s) \tilde{\mu}(X_s) + \tilde{\mu}''(X_s) (\tilde{\mu}(X_s))^2 \right) \int_s^t \int_s^u \int_s^r dv dr \circ dB_r^{\mathbb{P}} du \\ &+ \left(\tilde{\mu}'(X_s) \sigma'(X_s) \sigma(X_s) + \tilde{\mu}''(X_s) (\sigma(X_s))^2 \right) \int_s^t \int_s^u \int_s^r \circ dB_v^{\mathbb{P}} \circ dB_r^{\mathbb{P}} du \\ &+ \left(\tilde{\mu}'(X_s) \sigma'(X_s) \sigma(X_s) + \tilde{\mu}''(X_s) \sigma(X_s) \tilde{\mu}(X_s) \right) \int_s^t \int_s^u \int_s^r \circ dB_v^{\mathbb{P}} \circ dB_v^{\mathbb{P}} dr \circ dB_u^{\mathbb{P}} \\ &+ \left((\tilde{\mu}'(X_s))^2 \tilde{\mu}(X_s) + \sigma''(X_s) \sigma(X_s) \tilde{\mu}(X_s) \right) \int_s^t \int_s^u \int_s^r odB_v^{\mathbb{P}} \circ dB_v^{\mathbb{P}} \circ dB_u^{\mathbb{P}} \\ &+ \left((\sigma'(X_s))^2 \tilde{\mu}(X_s) + \sigma''(X_s) \sigma(X_s) \tilde{\mu}(X_s) \right) \int_s^t \int_s^u \int_s^r odB_v^{\mathbb{P}} \circ dB_v^{\mathbb{P}} \circ dB_u^{\mathbb{P}} \end{aligned}$$

$$+\underbrace{\varepsilon^{\tilde{\mu}} \int_{s}^{t} du + \varepsilon^{\sigma} \int_{s}^{t} \circ dB_{u}^{\mathbb{P}} + \tilde{\varepsilon}^{\tilde{\mu},\sigma}}_{s},\tag{32}$$

where we denote $\tilde{\varepsilon}^{\tilde{\mu},\sigma}$ as the collection of all the higher order error terms from double and triple integrals. We denote $\varepsilon^{\tilde{\mu},\sigma}:=\varepsilon^{\tilde{\mu}}\int_0^t ds + \varepsilon^{\sigma}\int_0^t \circ dB_s^{\mathbb{P}} + \tilde{\varepsilon}^{\tilde{\mu},\sigma}$ as the overall error term from the above expansion. This completes the proof.

3.3 Proof of Step 4.

Proof. Applying Girsanov theorem, plugging the dynamic $dB_t^{\mathbb{P}} = dB_t^{\mathbb{Q}} - \frac{\mu(X_t)}{\sigma(X_t)}dt$ into the expanison (32) from Step 3, we have

$$X_{t} = X_{s} + \tilde{\mu}(X_{s}) \int_{s}^{t} du + \sigma(X_{s}) \int_{s}^{t} \circ \left(dB_{u}^{\mathbb{Q}} - \frac{\mu(X_{u})}{\sigma(X_{u})} du\right) + \tilde{\mu}'(X_{s})\tilde{\mu}(X_{s}) \int_{s}^{t} \int_{s}^{u} dr du$$

$$+ \tilde{\mu}'(X_{s})\sigma(X_{s}) \int_{s}^{t} \int_{s}^{u} \circ \left(dB_{v}^{\mathbb{Q}} - \frac{\mu(X_{v})}{\sigma(X_{v})} dr\right) du + \sigma'(X_{s})\tilde{\mu}(X_{s}) \int_{s}^{t} \int_{s}^{u} dr \circ \left(dB_{u}^{\mathbb{Q}} - \frac{\mu(X_{u})}{\sigma(X_{u})} du\right)$$

$$+ \sigma'(X_{s})\sigma(X_{s}) \int_{s}^{t} \int_{s}^{u} \circ \left(dB_{v}^{\mathbb{Q}} - \frac{\mu(X_{v})}{\sigma(X_{v})} dr\right) \circ \left(dB_{u}^{\mathbb{Q}} - \frac{\mu(X_{u})}{\sigma(X_{u})} du\right)$$

$$+ \left((\tilde{\mu}'(X_{s}))^{2}\tilde{\mu}(X_{s}) + \tilde{\mu}''(X_{s})(\tilde{\mu}(X_{s}))^{2}\right) \int_{s}^{t} \int_{s}^{u} \int_{s}^{r} dv dr du$$

$$+ \left((\tilde{\mu}'(X_{s}))^{2}\sigma(X_{s}) + \tilde{\mu}''(X_{s})\tilde{\mu}(X_{s})\sigma(X_{s})\right) \int_{s}^{t} \int_{s}^{u} \int_{s}^{r} dv \circ \left(dB_{v}^{\mathbb{Q}} - \frac{\mu(X_{v})}{\sigma(X_{v})} dv\right) dr du$$

$$+ \left(\tilde{\mu}'(X_{s})\sigma'(X_{s})\tilde{\mu}(X_{s}) + \tilde{\mu}''(X_{s})\tilde{\mu}(X_{s})\sigma(X_{s})\right) \int_{s}^{t} \int_{s}^{u} \int_{s}^{r} dv dr \circ \left(dB_{v}^{\mathbb{Q}} - \frac{\mu(X_{v})}{\sigma(X_{v})} dr\right) du$$

$$+ \left(\tilde{\mu}'(X_{s})\sigma'(X_{s})\tilde{\mu}(X_{s}) + \tilde{\mu}''(X_{s})(\tilde{\mu}(X_{s}))^{2}\right) \int_{s}^{t} \int_{s}^{u} \int_{s}^{r} o ddB_{v}^{\mathbb{Q}} - \frac{\mu(X_{v})}{\sigma(X_{v})} dv\right) \circ \left(dB_{v}^{\mathbb{Q}} - \frac{\mu(X_{v})}{\sigma(X_{v})} dr\right) du$$

$$+ \left(\tilde{\mu}'(X_{s})\sigma'(X_{s})\sigma(X_{s}) + \tilde{\mu}''(X_{s})\sigma(X_{s})\tilde{\mu}(X_{s})\right) \int_{s}^{t} \int_{s}^{u} \int_{s}^{r} o \left(dB_{v}^{\mathbb{Q}} - \frac{\mu(X_{v})}{\sigma(X_{v})} dv\right) \circ \left(dB_{v}^{\mathbb{Q}} - \frac{\mu(X_{v})}{\sigma(X_{v})} dr\right) du$$

$$+ \left((\sigma'(X_{s}))^{2}\tilde{\mu}(X_{s}) + \sigma''(X_{s})\sigma(X_{s})\tilde{\mu}(X_{s})\right) \int_{s}^{t} \int_{s}^{u} \int_{s}^{r} dv \circ \left(dB_{v}^{\mathbb{Q}} - \frac{\mu(X_{v})}{\sigma(X_{v})} dv\right) dr \circ \left(dB_{u}^{\mathbb{Q}} - \frac{\mu(X_{u})}{\sigma(X_{u})} du\right)$$

$$+ \left((\sigma'(X_{s}))^{2}\tilde{\mu}(X_{s}) + \sigma''(X_{s})(\sigma(X_{s}))^{2}\right) \int_{s}^{t} \int_{s}^{u} \int_{s}^{r} dv \circ \left(dB_{v}^{\mathbb{Q}} - \frac{\mu(X_{v})}{\sigma(X_{v})} dv\right) dr \circ \left(dB_{u}^{\mathbb{Q}} - \frac{\mu(X_{u})}{\sigma(X_{u})} du\right)$$

$$+ \left((\sigma'(X_{s}))^{2}\sigma(X_{s}) + \sigma''(X_{s})(\sigma(X_{s}))^{2}\right) \left(dB_{v}^{\mathbb{Q}} - \frac{\mu(X_{v})}{\sigma(X_{v})} dr\right) \circ \left(dB_{v}^{\mathbb{Q}} - \frac{\mu(X_{v})}{\sigma(X_{v})} dv\right) dr \circ \left(dB_{u}^{\mathbb{Q}} - \frac{\mu(X_{u})}{\sigma(X_{u})} du\right)$$

$$+ \left((\sigma'(X_{s}))^{2}\tilde{\mu}(X_{s}) + \sigma''(X_{s})(\sigma(X_{s}))^{2}\right) \left(dB_{v}^{\mathbb{Q}} - \frac{\mu(X_{v})}{\sigma(X_{v})} dv\right) \circ \left(dB_{v}^{\mathbb{Q}} - \frac{\mu(X_{v})}{\sigma($$

Note that for the Black-Scholes model, the linear constant drift and diffusion coefficient assumption ensures that $\frac{\mu(X_u)}{\sigma(X_u)} = \frac{\mu(X_s)}{\sigma(X_s)}$ for all $u \in [s,t)$. In the spirit of Black-Sholes, we propose further approximation of $\frac{\mu(X_u)}{\sigma(X_u)}$ by $\frac{\mu(X_s)}{\sigma(X_s)}$ for the interval [s,t), and we denote $\varepsilon^{\mu/\sigma}$ as the error term from this approximation. This ensures some cancellations. Higher approximations of $\frac{\mu(X_u)}{\sigma(X_u)}$ is also possible here; we leave this for future studies. To derive the third-order approximation, we only collect the integrals with order $|t-s|^{3/2}$ terms in the above expansion, leaving all the higher terms in the error term. With a slight abuse of notation, we denote by $\varepsilon^{\mu,\sigma}$ the error term associated with the Taylor expansion for functions $\tilde{\mu}$ and σ , and by $\varepsilon^{\mu/\sigma}$ the error term associated with the approximation for $\frac{\mu}{\sigma}$. The final result after truncating to a third-order iterated integral and replacing $\frac{\mu(X_u)}{\sigma(X_u)}$ by the starting point $\frac{\mu(X_s)}{\sigma(X_s)}$ will be as follows.

$$X_{t} = X_{s} - \frac{1}{2}\sigma(X_{s})\sigma'(X_{s}) \int_{s}^{t} du + \sigma(X_{s}) \int_{s}^{t} \circ dB_{u}^{\mathbb{Q}}$$

$$+ \left(\mu'(X_{s})\sigma(X_{s}) - \mu(X_{s})\sigma'(X_{s}) - \frac{1}{2}\sigma(X_{s})\sigma'(X_{s})^{2} - \frac{1}{2}\sigma(X_{s})^{2}\sigma''(X_{s})\right) \int_{s}^{t} \int_{s}^{u} \circ dB_{r}^{\mathbb{Q}} du$$

$$- \frac{1}{2}\sigma(X_{s})\sigma'(X_{s})^{2} \int_{0}^{t} \int_{0}^{s} du \circ dB_{s}^{\mathbb{Q}} + \sigma'(X_{s})\sigma(X_{s}) \int_{s}^{t} \int_{s}^{u} \circ dB_{r}^{\mathbb{Q}} \circ dB_{u}^{\mathbb{Q}}$$

$$+\left(\left(\sigma'(X_s)\right)^2\sigma(X_s)+\sigma''(X_s)(\sigma(X_s))^2\right)\int_s^t\int_s^u\int_s^r\circ dB_v^{\mathbb{Q}}\circ dB_r^{\mathbb{Q}}\circ dB_u^{\mathbb{Q}}+\varepsilon^{\tilde{\mu},\sigma}+\varepsilon^{\mu/\sigma}.$$

The overall error terms $\varepsilon^{\tilde{\mu},\sigma} + \varepsilon^{\mu/\sigma}$ has the same order as $|t-s|^{2-\varepsilon}$, which is small if |t-s| is small. The proof is thus finished.

3.4 Proof of Step 5

Proof. Comparing the coefficients of (20) from Step 2 and (23) from Step 4, for the expansion of X_t at the initial point X_s on interval [s,t), we have the following equalities,

$$\begin{cases}
-\frac{1}{2}\sigma(X_s)\sigma'(X_s) = \psi_1^{s,t}, & \sigma(X_s) = \psi_2^{s,t}, & -\frac{1}{2}\sigma(X_s)\sigma'(X_s)^2 = \psi_{12}^{s,t} \\
\mu'(X_s)\sigma(X_s) - \mu(X_s)\sigma'(X_s) - \frac{1}{2}\sigma(X_s)\sigma'(X_s)^2 - \frac{1}{2}\sigma(X_s)^2\sigma''(X_s) = \psi_{21}^{s,t}, \\
\sigma(X_s)\sigma'(X_s) = \psi_{22}^{s,t}.
\end{cases} (34)$$

As we already get the values/functions of σ from step 1, we only focus on the function μ here. The equation associated with $\psi_{21}^{s,t}$ implies that

$$\mu'(X_s)\sigma(X_s) - \mu(X_s)\sigma'(X_s) - \frac{1}{2}\sigma(X_s)\sigma'(X_s)^2 - \frac{1}{2}\sigma(X_s)^2\sigma''(X_s) = \psi_{21}^{s,t}.$$
 (35)

Following the above observation, the parameter $\psi_{21}^{t_i,t_{i+1}}$ can be found corresponding to the initial value X_{t_i} , for $i=0,1,2,\cdots,n$. With this, the equation (35) holds true for each $t_i, i=0,1,2,\ldots,n$. For example, Eq. (35) equivalently written as

$$\mu'(X_{t_i})\sigma(X_{t_i}) - \mu(X_{t_i})\sigma'(X_{t_i}) - \frac{1}{2}\sigma(X_{t_i})\sigma'(X_{t_i})^2 - \frac{1}{2}\sigma(X_{t_i})^2\sigma''(X_{t_i}) = \psi_{21}^{t_i,t_{i+1}}, \quad \forall i = 0, 1, 2, \dots, n \quad (36)$$

This equation can be written compactly as

$$\mu'(X_r) = a(X_r)\mu(X_r) + b(X_r),$$
(37)

where $a(X_r) = \frac{\sigma'(X_r)}{\sigma(X_r)}$ and $b(X_r) = \frac{2\psi_{21}^{t_i,t_{i+1}} + \sigma(X_r)\sigma'(X_r)^2 + \sigma(X_r)^2\sigma''(X_r)}{2\sigma(X_r)}$, for $r \in [t_i,t_{i+1})$. Finally, if we know $\mu(X_0)$, and equation (37) has a unique solution for each interval $[t_i,t_{i+1})$, then we can solve the ODE using the simple Euler scheme as follows

$$\mu(X_{t_i}) = \mu(X_{t_{i-1}}) + \left[a(X_{t_{i-1}})\mu(X_{t_{i-1}}) + b(X_{t_{i-1}})\right](X_{t_i} - X_{t_{i-1}}), \quad \forall i = 1, 2, \dots, n.$$

Thus, the solution of the above ODE for each interval $[t_i, t_{i+1})$ can be used to construct estimators of the values of $\mu(X_{t_i})$ for $i = 1, \dots, N$. The proof is thus finished.

4 Numerical Experiments

4.1 Model description

In this section, we demonstrate the performance of our method for estimating the drift, diffusion function, and noise vector across several numerical examples. We assume the process X_t satisfies the dynamics as given in Eq. (5). We simulate sample paths using a standard time-discretization scheme, such as the Euler–Maruyama. With access to the data we compute its quadratic variation $[X]_{\pi,t_i}$ for each time index $t_i: 0 \le i \le n$ where $t_0 = 0, t_n = T, n = 100000$, and T = 1 of a chosen uniform partition π . The quadratic variation satisfies the ordinary differential equation $d[X]_{\pi,t} = (\sigma(X_t))^2 dt$. On estimated $Y_t = [X]_{\pi,t}$, we solve the regression problem (18) to get the functional form of $(\sigma(X_t))^2$ and hence $\sigma(X_t)$. The L_0 penalty $\|\Xi_{\sigma}\|_0$ in Eq. (18) induces sparsity, but since we focus only on estimating $\sigma(X_t)$ accurately, no regularization coefficient is included. We know that under risk-neutral probability \mathbb{Q} , the dynamics of X_t satisfy $dX_t = \sigma(X_t)dB_t^{\mathbb{Q}}$, which can be used to get the $B_t^{\mathbb{Q}}$ vector assuming it starts at zero. Now we have access to the primary process $(t_i, B_{t_i}^{\mathbb{Q}})$ for $0 \le i \le n$. We extend the features by using the idea of the iterated Stratonovich integral of the primary process up to order $|t-s|^{2-\epsilon}$ i.e., the integrals corresponding to the following coefficients

$$\Psi_2 := \{\psi_1, \psi_2, \psi_{12}, \psi_{21}, \psi_{22}, \psi_{222}\}.$$

We choose a sub-partition $\{j_k\}_{k=0}^M$, M << N of the partition π such that $t_{j_0} = t_0, t_{j_M} = t_N$ with M = 1000. On each sub-interval $[t_{j_k}, t_{j_{k+1}}]$ of this sub-partition X is regressed against above features to estimate the values of coefficients in the Ψ_2 at $t = t_{j_k}$ for $k = 0, \ldots, M$. The ODE (24) is then solved to get the vector of $\mu(X_{t_{j_k}})$ for each t_{j_k} . Furthermore, we use the discretization scheme (25) to predict the noise increment vectors $(\Delta B_{t_{j_0}}^{\mathbb{P}}, \Delta B_{t_{j_1}}^{\mathbb{P}}, \cdots, \Delta B_{t_{j_M}}^{\mathbb{P}})$ hence the noise $B^{\mathbb{P}}$ by assuming it starts at zero. Finally, we use the SSISDE (28) to recover the symbolic form of drift $\mu(X_t)$ and diffusion $\sigma(X_t)$. We describe the model-selection procedure, i.e., k-fold time-series cross-validation, the CV error δ , and the choice of the optimal sparsity level, before presenting the numerical examples.

4.1.1 Model selection via k-fold time-series cross-validation

We adopt an elastic-net penalty Hastie et al. (2009) in the penalized identification problem (28), namely

$$\mathcal{R}_{\alpha,\rho}(\Xi_{\mu},\Xi_{\sigma}) = \alpha \left(\rho \|\beta\|_{1} + \frac{1-\rho}{2} \|\beta\|_{2}^{2}\right), \qquad \beta := \begin{bmatrix} \Xi_{\mu} \\ \Xi_{\sigma} \end{bmatrix},$$

with $\|\cdot\|_1$ and $\|\cdot\|_2$ the usual vector norms. The penalty strength $\alpha>0$ and mixing parameter $\rho\in[0,1]$ are hyperparameters that control sparsity and shrinkage in (Ξ_μ,Ξ_σ) ($\rho=1$ recovers Lasso; $\rho=0$ Ridge). We select (α,ρ) by k-fold time-series cross-validation Stone (1974) (no shuffling across time): let $\{A_j\}_{j=1}^k$ partition the index set $\{1,\ldots,N-1\}$ into k contiguous, non-overlapping validation blocks, and define $B_j:=\bigcup_{\ell\neq j}A_\ell$ as the complementary training indices. For each candidate pair (α,ρ) and each fold j, we fit (28) on B_j to obtain $(\widehat{\Xi}_\mu^{(j)},\widehat{\Xi}_\sigma^{(j)})$, and compute the mean squared one-step prediction error on A_j :

$$\delta_j^2(\alpha, \rho) := \frac{1}{|A_j|} \sum_{i \in A_i} \left\| \Delta X_{t_i} - \Theta_\mu(X_{t_i}) \, \widehat{\Xi}_\mu^{(j)} \, \Delta t_i - \Theta_\sigma(X_{t_i}) \, \widehat{\Xi}_\sigma^{(j)} \, \Delta B_{t_i}^{\mathbb{P}} \right\|_2^2.$$

The k-fold CV score and its standard error are

$$\overline{\delta}(\alpha,\rho) = \frac{1}{k} \sum_{j=1}^{k} \delta_j(\alpha,\rho), \qquad \text{SE}(\alpha,\rho) = \sqrt{\frac{1}{k(k-1)} \sum_{j=1}^{k} (\delta_j(\alpha,\rho) - \overline{\delta}(\alpha,\rho))^2}.$$

We evaluate $\bar{\delta}$ on a logarithmic grid $\alpha \in \Lambda$ and a discrete set $\rho \in \mathcal{P}$ (including $\rho = 1$ for Lasso). To reduce shrinkage bias, after solving (28) on each training fold we refit an ordinary least-squares model restricted to the active set (nonzero entries of $(\widehat{\Xi}_{\mu}^{(j)}, \widehat{\Xi}_{\sigma}^{(j)})$) before scoring on A_j .

4.1.2 Choice of the final model

Let $(\alpha_{\star}, \rho_{\star}) = \arg \min_{\alpha, \rho} \bar{\delta}(\alpha, \rho)$ and define the one-standard-error Hastie et al. (2009) threshold

$$\varepsilon = \overline{\delta}(\alpha_{\star}, \rho_{\star}) + SE(\alpha_{\star}, \rho_{\star}).$$

Among all (α, ρ) with $\bar{\delta}(\alpha, \rho) \leq \varepsilon$, we pick the *simplest* model, i.e., the one with the smallest support size (fewest nonzeros in $(\Xi_{\mu}, \Xi_{\sigma})$); ties are broken toward larger α (and larger ρ when applicable). This yields $(\alpha^{\dagger}, \rho^{\dagger})$ and the corresponding $(\widehat{\Xi}_{\mu}, \widehat{\Xi}_{\sigma})$. We then refit (28) on the *full* dataset with $(\alpha^{\dagger}, \rho^{\dagger})$, followed by the same restricted least-squares de-biasing on the selected support, and we report the in-sample mean squared error as a summary of fit quality.

4.1.3 Optimally sparse size

It is often informative to summarize CV results as a function of the active-set sizes

$$n_{\mu} := \|\widehat{\Xi}_{\mu}\|_{0}, \qquad n_{\sigma} := \|\widehat{\Xi}_{\sigma}\|_{0},$$

where $\|\cdot\|_0$ counts nonzero entries [see e.g. Efron et al. (2004), Boninsegna et al. (2018)]. Grouping all grid points (α, ρ) that yield the same $n \in \mathbb{N}$, define

$$\delta(n) = \min_{\substack{(\alpha,\rho): \|\widehat{\Xi}\|_{0} = n}} \overline{\delta}(\alpha,\rho), \qquad \widehat{\Xi} := (\widehat{\Xi}_{\mu}, \widehat{\Xi}_{\sigma}).$$

Empirically, $\delta(n)$ typically exhibits three regimes: (i) underfitting at very small n (large error), (ii) a flat "good" region where accuracy is stable across several n, and (iii) overfitting at very large n (rising error). We define the *optimally sparse* sizes $\tilde{n}_{\mu}, \tilde{n}_{\sigma}$ as the smallest n whose error lies within one standard error of the minimum of $\delta(n)$ (a size-based analogue of the 1-SE rule). We compare them with the sizes actually selected by $(\alpha^{\dagger}, \rho^{\dagger})$. For completeness we also provide " δ vs. n" plots with ± 1 SE bands for both μ and σ .

⁵All feature normalizations are computed using training data of each fold only and then applied to both training and validation rows to prevent temporal leakage.

4.1.4 Practical settings used in our experiments

Unless stated otherwise, we use k=7 contiguous folds, a logarithmic grid $\Lambda = \{\alpha_{\min}, \dots, \alpha_{\max}\}$ spanning several decades for α , and $\mathcal{P} = \{0.3, 0.4, 0.5, 0.7, 0.85, 0.95, 1.0\}$ for ρ (with $\rho = 1.0$ recovering Lasso). Feature blocks are built as

$$\Theta_{\mu}(X_{t_i}) \Delta t_i$$
 and $\Theta_{\sigma}(X_{t_i}) \Delta B_{t_i}^{\mathbb{P}}$,

with RMS column normalization applied separately to each block on the training portion of each fold. All reported coefficients are de-biased by restricted least squares on the selected support. Alongside $(\alpha^{\dagger}, \rho^{\dagger})$ and $(\tilde{n}_{\mu}, \tilde{n}_{\sigma})$, we provide the final model size, validation curves/surfaces, and δ vs. n summaries to document the sparsity–accuracy trade-off achieved by (28) in each example. Finally, let us discuss the results of our numerical experiments in the case of different classical examples.

4.2 Black-Scholes model

Consider the Black-Scholes SDE

$$dX_t = \mu \ X_t \ dt + \sigma \ X_t \ dB_t^{\mathbb{P}},$$

where μ and $\sigma > 0$ are two constants, and the solution is a Geometric Brownian motion. This is an example of an SDE that does not satisfy the ergodicity assumption. It is the widely used dynamics for stock prices in finance. The idea traces back to Osborne and Samuelson's lognormal price hypothesis Osborne (1959) and was formalized in the Black–Scholes–Merton framework Black and Scholes (1973) as geometric Brownian motion. The drift term is linear in the price, μX_t , and shows a proportional (percentage) expected rate of return. The diffusion term is also linear, $\sigma X_t dB_t^{\mathbb{P}}$, and σ is taken positive because it represents standard deviation, and any negative sign can be absorbed by flipping the Brownian motion. In short, the drift part governs the systematic trend while the diffusion part quantifies how volatile the price is around that trend.

For our numerical experiment we simulate X_t by taking

$$\mu(X_t) = 0.5X_t$$
, and $\sigma(X_t) = 0.3X_t$.

To identify the Black–Scholes drift, diffusion function, and noise from a single path using the penalized residual (28). We take polynomial libraries for both blocks, $\Theta_{\mu}(x) = \{1, x, \dots, x^5\}$ and $\Theta_{\sigma}(x) = \{1, x, \dots, x^5\}$, and tune (α, ρ) by k-fold time–series CV with k = 7 on a log grid for α and a discrete set for ρ , with de-biasing on the active set and the 1-SE rule for parsimony. The CV surface/curves select an Elastic–Net point

$$\alpha^{\dagger} \approx 3.87 \times 10^{-4}, \qquad \rho^{\dagger} = 0.85,$$

lying in a broad near-optimal region (Fig. 1). At these hyperparameters, the recovered laws are

$$\widehat{\mu}(x) = 0.503681 \, x, \qquad \widehat{\sigma}(x) = 0.00241444 + 0.296498 \, x,$$

with one–step MSE = 5.275×10^{-9} . Thus, the drift is identified as purely proportional (support size $n_{\mu} = 1$), and the diffusion is essentially linear with a small intercept (support size $n_{\sigma} = 2$). The δ –vs–n summaries place the chosen sizes at the left edge of the flat accuracy region, indicating no material gain from adding higher-order terms (Fig. 2). The four-panel diagnostic shows that $\hat{\mu}(X_t)$ and $\hat{\sigma}(X_t)$ track the true trajectories closely, the recovered noise overlaps the driving process, and the simulated path is visually indistinguishable from the observed X_t (Fig. 3). Overall, the identification is faithful to the Black–Scholes structure while remaining parsimonious.

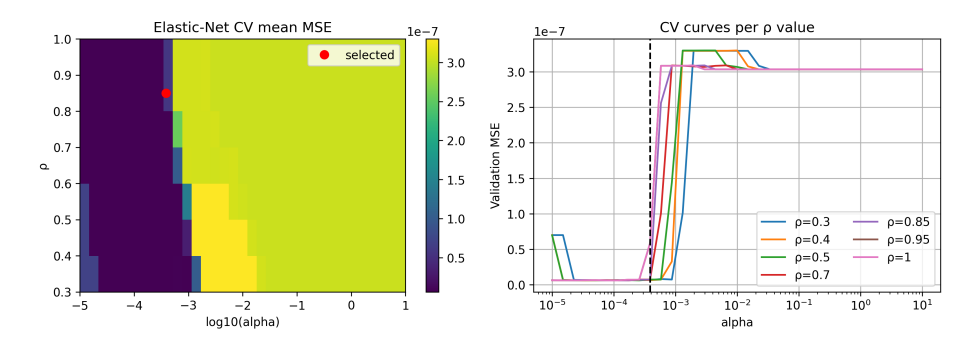


Figure 1: Time-series CV over (α, ρ) with de-biasing on the active set; the selected point $(\alpha^{\dagger}, \rho^{\dagger}) = (3.87 \times 10^{-4}, 0.85)$ lies on a broad near-optimal basin.

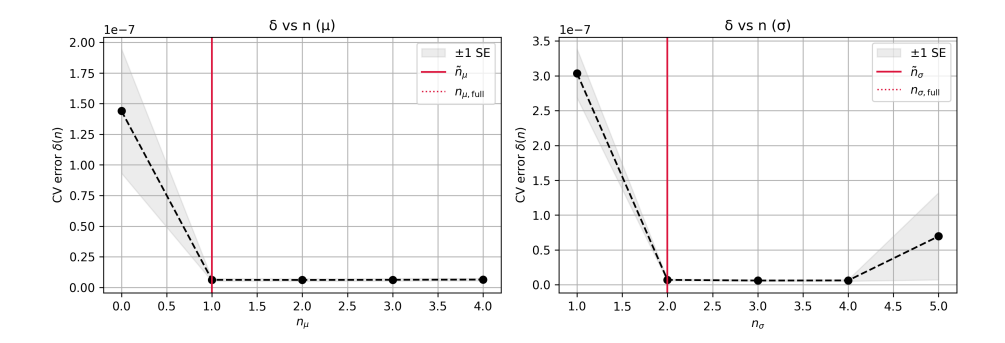


Figure 2: Validation error $\delta(n)$ vs. support size n with ± 1 SE bands for the drift and diffusion blocks. The vertical markers indicate the optimally sparse sizes and the sizes of the final full-data models.

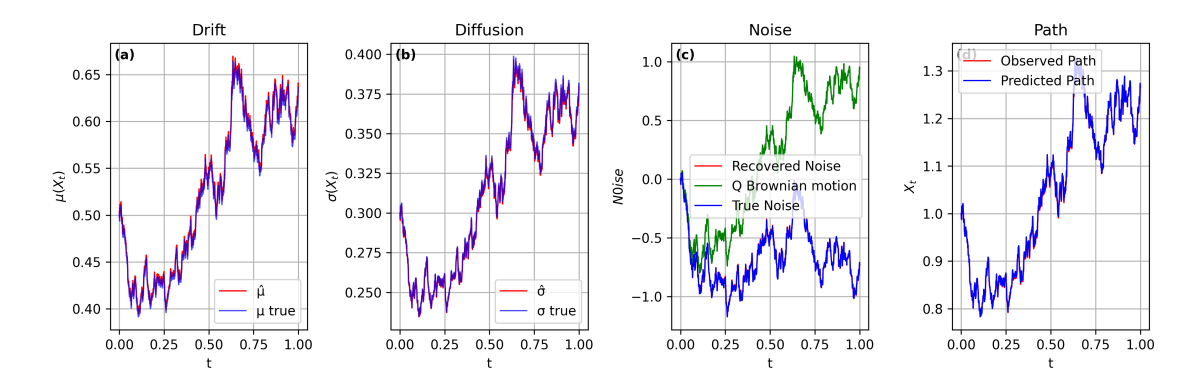


Figure 3: (a) The true $\mu(X_t)$ and reconstructed $\widehat{\mu}(X_t)$ and (b) The true $\sigma(X_t)$ and reconstructed $\widehat{\sigma}(X_t)$ are plotted against time on the interval [0,1]. (c) The true noise, i.e., Brownian motion $B^{\mathbb{P}}$ that was used to simulate the actual path, the recovered noise, and the \mathbb{Q} -Brownian motion are plotted against time. (d) The actual path of the data X_t and the reconstructed one from the $\widehat{\mu}(X_t)$ and $\widehat{\sigma}(X_t)$ are plotted against time. Each vector is of length M with M = 1000.

4.3 Quadratic coefficients SDE

In this example, we study the SDE with quadratic drift and diffusion,

$$dX_t = \underbrace{\left(0.7X_t + 0.3X_t^2\right)}_{\mu(X_t)} dt + \underbrace{\left(0.5X_t + 0.1X_t^2\right)}_{\sigma(X_t)} dB_t^{\mathbb{P}}, \tag{38}$$

which belongs to the broader class of polynomial/CEV-type diffusions Davydov and Linetsky (2001). Unlike geometric Brownian motion, (38) features state-dependent nonlinearities in *both* the drift and the diffusion.

We illustrate the full identification pipeline on this one-dimensional SDE and recover both the drift and diffusion function from a single trajectory via the penalized residual (28). The feature libraries for drift and diffusion are polynomial dictionaries

$$\Theta_{\mu}(x) = \{1, x, x^2, x^3, x^4, x^5\}, \qquad \Theta_{\sigma}(x) = \{1, x, x^2, x^3, x^4, x^5\},$$

so that the analytic basis functions used to generate the data are the first two non-constant monomials $[x, x^2]$ in each dictionary. Hyperparameters (α, ρ) are selected by k-fold time–series cross-validation with k = 7, using a logarithmic grid $\alpha \in \{\text{geomspace}(10^{-5}, 10^1, 35)\}$ and $\rho \in \{0.3, 0.4, 0.5, 0.7, 0.85, 0.95, 1.0\}$. After each penalized fit on the training folds, we de-bias by restricted least squares on the active support before scoring on the validation fold, and apply the 1-SE rule to favor parsimony.

The CV surface/curves in Fig. 4 show a broad near-optimal basin around $\alpha \sim 10^{-3}$ for $\rho \in [0.4, 0.7]$. The 1-SE rule selects an Elastic–Net model at

$$\alpha^{\dagger} \approx 8.73 \times 10^{-4}, \qquad \rho^{\dagger} = 0.50,$$

marked in the figure. This choice lies on the left edge of the plateau and yields a sparse, stable model with validation error statistically indistinguishable from the minimum.

Aggregating CV outcomes by support size $n = \|(\Xi_{\mu}, \Xi_{\sigma})\|_0$ produces the characteristic $\delta(n)$ profile in Fig. 5: a sharp drop from the underfit regime, a flat region of near-minimal error, and a mild rise at larger supports. The vertical markers show the optimally sparse sizes \tilde{n} returned by the 1-SE rule together with the sizes of the final full-data models. In our run, the chosen model sits at the left boundary of the flat region, indicating that additional nonzeros do not materially improve validation error, whereas removing one more term increases δ noticeably.

Finally, fitting (28) on the full dataset with $(\alpha^{\dagger}, \rho^{\dagger})$ and de-biasing on the selected support yields

$$\widehat{\mu}(x) = 0.620512 \, x + 0.35905 \, x^2, \qquad \widehat{\sigma}(x) = -0.017782 + 0.535985 \, x + 0.0842435 \, x^2,$$

with one–step MSE 1.448×10^{-7} (Fig. 6). The drift support matches the analytic basis $\{x, x^2\}$ and displays small coefficient biases. The diffusion includes a small intercept and mild biases on the linear and quadratic terms.

The four-panel summary in Fig. 6 confirms dynamical exactitude: (a) $\widehat{\mu}(X_t)$ overlays the true drift trajectory with tiny residuals; (b) $\widehat{\sigma}(X_t)$ tracks the true diffusion across the explored state range; (c) the recovered noise closely matches both the driving process $B^{\mathbb{P}}$ with little monotonic deviation from \mathbb{Q} Brownian motion which is consistent with the theory; (d) simulating with $(\widehat{\mu}, \widehat{\sigma})$ reproduces the observed path X_t , and the predicted path is visually indistinguishable at plot scale. Together with the very small MSE, these diagnostics indicate that the method has captured the correct functional structure.

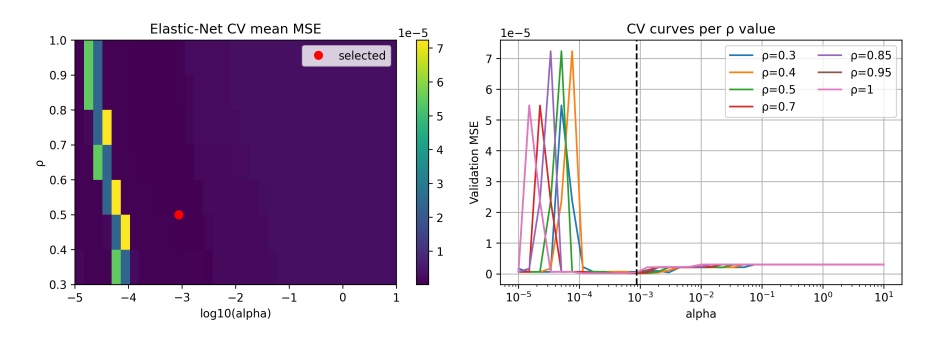


Figure 4: Time-series cross-validation over (α, ρ) with de-biasing on the active set. The selected point $(\alpha^{\dagger}, \rho^{\dagger}) = (8.73 \times 10^{-4}, 0.50)$ lies on a broad plateau of optimal values.

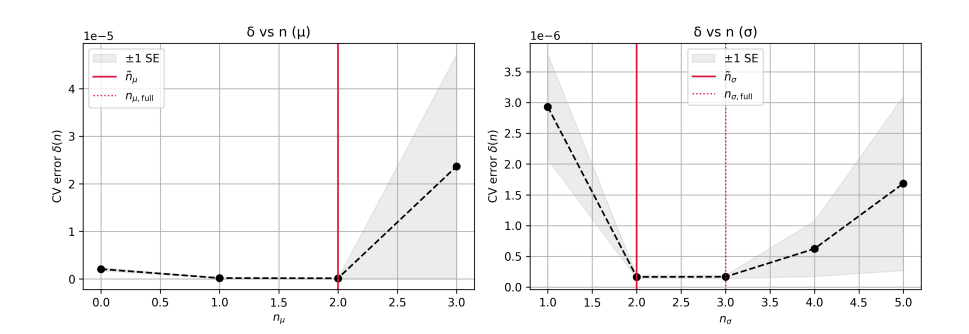


Figure 5: Validation error $\delta(n)$ vs. support size n with ± 1 SE bands. Vertical lines indicate the optimally sparse sizes \tilde{n} (1-SE rule) and the final full-data sizes.

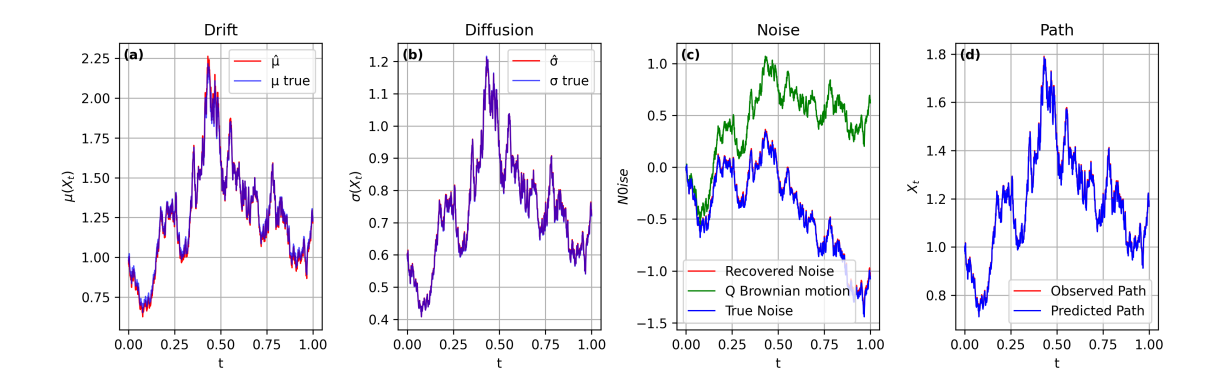


Figure 6: (a) The true $\mu(X_t)$ and reconstructed $\widehat{\mu}(X_t)$ and (b) The true $\sigma(X_t)$ and reconstructed $\widehat{\sigma}(X_t)$ are plotted against time on the interval [0,1]. (c) The true noise, i.e., Brownian motion $B^{\mathbb{P}}$ that was used to simulate the actual path, the predicted noise, and the \mathbb{Q} -Brownian motion are plotted against time. (d) The actual path of the data X_t and the reconstructed one from the $\widehat{\mu}(X_t)$ and $\widehat{\sigma}(X_t)$ are plotted against time. Each vector is of length M with M = 1000.

References

Aït-Sahalia, Y. (2002). Maximum likelihood estimation of discretely sampled diffusions: A closed-form approximation approach. *Econometrica*, 70(1):223–262.

Anderson, T. W. (1959). On asymptotic distributions of estimates of parameters of stochastic difference equations. *The Annals of Mathematical Statistics*, 30(3):676–687.

Arribas, I. P. (2018). Derivatives pricing using signature payoffs. arXiv preprint arXiv:1809.09466.

Azencott, R. (2006). Formule de taylor stochastique et développement asymptotique d'intégrales de feynmann. In Séminaire de Probabilités XVI, 1980/81 Supplément: Géométrie Différentielle Stochastique, pages 237—285. Springer.

Aït-Sahalia, Y. (1996). Nonparametric pricing of interest rate derivative securities. *Econometrica*, 64(3):527–560.

Bai, Z., Brunton, S. L., Brunton, B. W., Kutz, J. N., Kaiser, E., Spohn, A., and Noack, B. R. (2017). Data-driven methods in fluid dynamics: Sparse classification from experimental data. Springer.

Bayer, C., Hager, P. P., Riedel, S., and Schoenmakers, J. (2023). Optimal stopping with signatures. *The Annals of Applied Probability*, 33(1):238–273.

Bibby, B. M. and Sørensen, M. (1995). Martingale estimation functions for discretely observed diffusion processes. *Bernoulli*, pages 17–39.

Black, F. and Scholes, M. (1973). The pricing of options and corporate liabilities. *Journal of political economy*, 81(3):637–654.

Bongard, J. and Lipson, H. (2007). Automated reverse engineering of nonlinear dynamical systems. *Proceedings of the National Academy of Sciences*, 104(24):9943–9948.

Boninsegna, L., Nüske, F., and Clementi, C. (2018). Sparse learning of stochastic dynamical equations. *The Journal of chemical physics*, 148(24).

Brunton, S. L., Proctor, J. L., and Kutz, J. N. (2016). Discovering governing equations from data by sparse identification of nonlinear dynamical systems. *Proceedings of the national academy of sciences*, 113(15):3932–3937.

Casella, G., Ghosh, M., Gill, J., and Kyung, M. (2010). Penalized regression, standard errors, and Bayesian lassos. *Bayesian Analysis*, 5(2):369 – 411.

Castell, F. (1993). Asymptotic expansion of stochastic flows. Probability theory and related fields, 96(2):225–239.

- Chen, Z., Liu, Y., and Sun, H. (2021). Physics-informed learning of governing equations from scarce data. Nature communications, 12(1):6136.
- Comte, F., Genon-Catalot, V., and Rozenholc, Y. (2007). Penalized nonparametric mean square estimation of the coefficients of diffusion processes. *Bernoulli*, 13(2):514–543.
- Cuchiero, C., Gazzani, G., Möller, J., and Svaluto-Ferro, S. (2025). Joint calibration to spx and vix options with signature-based models. *Mathematical Finance*, 35(1):161–213.
- Cuchiero, C., Gazzani, G., and Svaluto-Ferro, S. (2023). Signature-based models: theory and calibration. SIAM journal on financial mathematics, 14(3):910–957.
- Dacunha-Castelle, D. and Florens-Zmirou, D. (1986). Estimation of the coefficients of a diffusion from discrete observations. Stochastics: An International Journal of Probability and Stochastic Processes, 19(4):263–284.
- Dalalyan, A. and Reiß, M. (2007). Asymptotic statistical equivalence for ergodic diffusions: the multidimensional case. *Probability theory and related fields*, 137(1):25–47.
- Davydov, D. and Linetsky, V. (2001). Pricing and hedging path-dependent options under the cev process. *Management science*, 47(7):949–965.
- Duffie, D. and Glynn, P. (2004). Estimation of continuous-time markov processes sampled at random time intervals. *Econometrica*, 72(6):1773–1808.
- Efron, B., Hastie, T., Johnstone, I., and Tibshirani, R. (2004). Least angle regression. *The Annals of Statistics*, 32(2):407–499.
- Ermolaev, A. V., Sheveleva, A., Genty, G., Finot, C., and Dudley, J. M. (2022). Data-driven model discovery of ideal four-wave mixing in nonlinear fibre optics. *Scientific Reports*, 12(1):12711.
- Fan, J. and Zhang, C. (2003). A reexamination of diffusion estimators with applications to financial model validation. Journal of the American Statistical Association, 98(461):118–134.
- Florens-Zmirou, D. (1989). Approximate discrete-time schemes for statistics of diffusion processes. *Statistics:* A Journal of Theoretical and Applied Statistics, 20(4):547–557.
- Friedman, J., Hastie, T., and Tibshirani, R. (2010). A note on the group lasso and a sparse group lasso. arXiv preprint arXiv:1001.0736.
- Friz, P. K. and Victoir, N. B. (2010). Multidimensional Stochastic Processes as Rough Paths: Theory and Applications. Cambridge Studies in Advanced Mathematics. Cambridge University Press.
- Girsanov, I. V. (1960). On transforming a certain class of stochastic processes by absolutely continuous substitution of measures. *Theory of Probability & Its Applications*, 5(3):285–301.
- Hansen, L. P. and Scheinkman, J. A. (1993). Back to the future: Generating moment implications for continuous-time markov processes.
- Hansen, L. P., Scheinkman, J. A., and Touzi, N. (1998). Spectral methods for identifying scalar diffusions. Journal of Econometrics, 86(1):1–32.
- Harirchi, F., Kim, D., Khalil, O., Liu, S., Elvati, P., Baranwal, M., Hero, A., and Violi, A. (2020). On sparse identification of complex dynamical systems: A study on discovering influential reactions in chemical reaction networks. Fuel, 279:118204.
- Harrison, J. and Pliska, S. R. (1981). Martingales and stochastic integrals in the theory of continuous trading. Stochastic Processes and their Applications, 11(3):215–260.
- Hastie, T., Tibshirani, R., Friedman, J., et al. (2009). The elements of statistical learning.
- Kaptanoglu, A. A., Hansen, C., Lore, J. D., Landreman, M., and Brunton, S. L. (2023). Sparse regression for plasma physics. *Physics of Plasmas*, 30(3).
- Karatzas, I. and Shreve, S. E. (1991). Brownian Motion and Stochastic Calculus, volume 113 of Graduate Texts in Mathematics. Springer, New York, 2nd edition.
- Kessler, M. (1997). Estimation of an ergodic diffusion from discrete observations. Scandinavian Journal of Statistics, 24(2):211–229.

- Kidger, P. and Lyons, T. (2020). Signatory: differentiable computations of the signature and logsignature transforms, on both cpu and gpu. arXiv preprint arXiv:2001.00706.
- Kloeden, P. E. and Platen, E. (1992). Stochastic Taylor Expansions, pages 161–226. Springer Berlin Heidelberg, Berlin, Heidelberg.
- Koza, J. R. (1994). Genetic programming as a means for programming computers by natural selection. *Statistics and computing*, 4:87–112.
- Kutoyants, Y. A. (2013). Statistical inference for ergodic diffusion processes. Springer Science & Business Media.
- Lamouroux, D. and Lehnertz, K. (2009). Kernel-based regression of drift and diffusion coefficients of stochastic processes. *Physics Letters A*, 373(39):3507–3512.
- Lyons, T. and Victoir, N. (2004). Cubature on wiener space. Proceedings of the Royal Society of London. Series A: Mathematical, Physical and Engineering Sciences, 460(2041):169–198.
- Lyons, T. J. (1998). Differential equations driven by rough signals. Revista Matemática Iberoamericana, 14(2):215–310.
- Mangan, N. M., Brunton, S. L., Proctor, J. L., and Kutz, J. N. (2016). Inferring biological networks by sparse identification of nonlinear dynamics. *IEEE Transactions on Molecular, Biological, and Multi-Scale Communications*, 2(1):52–63.
- Mangan, N. M., Kutz, J. N., Brunton, S. L., and Proctor, J. L. (2017). Model selection for dynamical systems via sparse regression and information criteria. *Proceedings of the Royal Society A: Mathematical, Physical and Engineering Sciences*, 473(2204):20170009.
- Melino, A. (1994). Estimation of continuous time models in finance. *Journal of Financial economics*, 8:323–362.
- Merton, R. C. (1980). On estimating the expected return on the market: An exploratory investigation. *Journal of Financial Economics*, 8(4):323–361.
- Øksendal, B. (2003). Stochastic differential equations. In Stochastic differential equations: an introduction with applications, pages 38–50. Springer.
- Osborne, M. F. (1959). Brownian motion in the stock market. Operations research, 7(2):145-173.
- Rudy, S. H., Brunton, S. L., Proctor, J. L., and Kutz, J. N. (2017). Data-driven discovery of partial differential equations. *Science advances*, 3(4):e1602614.
- Schaeffer, H., Tran, G., and Ward, R. (2017). Learning dynamical systems and bifurcation via group sparsity. arXiv preprint arXiv:1709.01558.
- Schmidt, M. and Lipson, H. (2009). Distilling free-form natural laws from experimental data. *science*, 324(5923):81–85.
- Semnani, P., Guan, V., Robeva, E., and Lee, D. (2025). Path-dependent sdes: Solutions and parameter estimation.
- Stanton, R. (1997). A nonparametric model of term structure dynamics and the market price of interest rate risk. *The Journal of Finance*, 52(5):1973–2002.
- Stevens-Haas, J. M., Bhangale, Y., Kutz, J. N., and Aravkin, A. (2024). Learning nonlinear dynamics using kalman smoothing. *IEEE Access*.
- Stone, M. (1974). Cross-validatory choice and assessment of statistical predictions. *Journal of the royal statistical society: Series B (Methodological)*, 36(2):111–133.
- Udrescu, S.-M. and Tegmark, M. (2020). Ai feynman: A physics-inspired method for symbolic regression. *Science Advances*, 6(16):eaay2631.
- Wanner, M. and Mezić, I. (2024). On higher order drift and diffusion estimates for stochastic sindy. SIAM Journal on Applied Dynamical Systems, 23(2):1504–1539.
- Yuan, M. and Lin, Y. (2006). Model selection and estimation in regression with grouped variables. *Journal of the Royal Statistical Society Series B: Statistical Methodology*, 68(1):49–67.

- Zanna, L. and Bolton, T. (2020). Data-driven equation discovery of ocean mesoscale closures. Geophysical $Research\ Letters,\ 47(17)$:e2020GL088376.
- Zhang, S. and Lin, G. (2018). Robust data-driven discovery of governing physical laws with error bars. *Proceedings of the Royal Society A: Mathematical, Physical and Engineering Sciences*, 474(2217):20180305.